UNIVERSITY OF AMSTERDAM

UvA-DARE (Digital Academic Repository)

Search for high-mass Wγ and Zγ resonances using hadronic W/Z boson decays from 139 fb^{-1} of pp collisions at $\sqrt{s}$ = 13 TeV with the ATLAS detector

The ATLAS Collaboration

DOI
10.1007/JHEP07(2023)125

Publication date
2023

Document Version
Final published version

Published in
Journal of High Energy Physics

License
CC BY

Link to publication

Citation for published version (APA):
The ATLAS Collaboration (2023). Search for high-mass *Wγ* and *Zγ* resonances using hadronic *W/Z* boson decays from 139 fb^{-1} of *pp* collisions at $\sqrt{s}$ = 13 TeV with the ATLAS detector. *Journal of High Energy Physics*, *2023*(7), Article 125. https://doi.org/10.1007/JHEP07(2023)125

General rights
It is not permitted to download or to forward/distribute the text or part of it without the consent of the author(s) and/or copyright holder(s), other than for strictly personal, individual use, unless the work is under an open content license (like Creative Commons).

Disclaimer/Complaints regulations
If you believe that digital publication of certain material infringes any of your rights or (privacy) interests, please let the Library know, stating your reasons. In case of a legitimate complaint, the Library will make the material inaccessible and/or remove it from the website. Please Ask the Library: https://uba.uva.nl/en/contact, or a letter to: Library of the University of Amsterdam, Secretariat, P.O. Box 19185, 1000 GD Amsterdam, The Netherlands. You will be contacted as soon as possible.

UvA-DARE is a service provided by the library of the University of Amsterdam (https://dare.uva.nl)

Download date:07 Sept 2026

Published for SISSA by Springer

Received: *April 25, 2023*
Accepted: *July 3, 2023*
Published: *July 14, 2023*

Search for high-mass $W\gamma$ and $Z\gamma$ resonances using hadronic W/Z boson decays from 139 fb^{-1} of pp collisions at $\sqrt{s} = 13$ TeV with the ATLAS detector

The ATLAS collaboration

E-mail: atlas.publications@cern.ch

Abstract: A search for high-mass charged and neutral bosons decaying to $W\gamma$ and $Z\gamma$ final states is presented in this paper. The analysis uses a data sample of $\sqrt{s} = 13$ TeV proton-proton collisions with an integrated luminosity of 139 fb^{-1} collected by the ATLAS detector during LHC Run 2 operation. The sensitivity of the search is determined using models of the production and decay of spin-1 charged bosons and spin-0/2 neutral bosons. The range of resonance masses explored extends from 1.0 TeV to 6.8 TeV. At these high resonance masses, it is beneficial to target the hadronic decays of the W and Z bosons because of their large branching fractions. The decay products of the high-momentum W/Z bosons are strongly collimated and boosted-boson tagging techniques are employed to improve the sensitivity. No evidence of a signal above the Standard Model backgrounds is observed, and upper limits on the production cross-sections of these bosons times their branching fractions to $W\gamma$ and $Z\gamma$ are derived for various boson production models.

Keywords: Hadron-Hadron Scattering

ArXiv ePrint: 2304.11962

Open Access, Copyright CERN,
for the benefit of the ATLAS Collaboration.
Article funded by SCOAP^3.

https://doi.org/10.1007/JHEP07(2023)125

Contents

1 Introduction **1**

2 ATLAS detector **2**

3 Data collection and Monte Carlo event simulation **3**
3.1 Data samples 3
3.2 Monte Carlo simulation 3

4 Event reconstruction **5**
4.1 Particle reconstruction 5
4.2 Event selection and categorization 7

5 Signal and background modelling **9**
5.1 SM background modelling 10
5.2 BSM signal modelling 11

6 Systematic uncertainties **11**

7 Statistical analysis **13**

8 Results **15**

9 Conclusion **21**

The ATLAS collaboration **27**

JHEP07(2023)125

1 Introduction

Speculations about physics phenomena beyond those described by the Standard Model (SM) often result in the introduction of new bosons, due to either additional gauge symmetries or postulated extensions of the Higgs sector [1–3]. The high-energy proton-proton (pp) collisions provided by the Large Hadron Collider (LHC) make it possible to produce these new bosons with masses up to approximately one hundred times the mass of the SM W and Z bosons. A broad range of beyond-the-SM (BSM) scenarios can therefore be tested with experiments at the LHC that search for high-mass charged and neutral bosons.

Some of the BSM theories predict new charged $X^{\pm}$ and neutral X^{0} bosons [3, 4]. From an experimental perspective, $W\gamma$ or $Z\gamma$ final states are attractive since a high-energy photon signature efficiently selects signal events and rejects background. For bosons with masses of the order of TeV, decays of the type $X^{\pm} \to W^{\pm}\gamma$ or $X^{0} \to Z\gamma$ result in a highly boosted W or Z boson, where the decay products of such a boson are very collimated. This

analysis targets the hadronic decay modes of W and Z bosons to quark-antiquark pairs reconstructed as large-radius (large-R) jets that have a two-prong structure identified using jet-substructure information [5]. The complete reconstruction of the $W\gamma$ or $Z\gamma$ final state can then be used to determine the mass and other properties of the new bosons.

This paper presents searches for massive $X^{\pm}$ and X^0 bosons using 139 fb^{-1} of pp collisions at a centre-of-mass energy ($\sqrt{s}$) of 13 TeV recorded with the ATLAS detector. The searches assume that the decay width of the heavy bosons is small compared to the experimental resolution, but are otherwise generic, looking for any excess of events above smooth SM background $W\gamma$ and $Z\gamma$ invariant mass spectra. The measurements are compared with the predictions of models of the production and decay of spin-1 charged bosons and spin-0/2 neutral bosons. These include $q\bar{q}'$ annihilation production of spin-1 $X^{\pm} \to W^{\pm}\gamma$, gluon-gluon fusion production of spin-0 $X^0 \to Z\gamma$, and both gluon-gluon fusion and $q\bar{q}$ annihilation production of spin-2 $X^0 \to Z\gamma$. A boson mass (m_X) range from 1.0 to 6.8 TeV is covered by these searches.

Previous searches for bosons of mass greater than 1.0 TeV decaying to $W\gamma$ and $Z\gamma$ final states have been carried out at the LHC by the ATLAS [6–8] and CMS [9–12] Collaborations. Compared to the previous ATLAS search based on 36.1 fb^{-1} of Run 2 $\sqrt{s} = 13$ TeV pp collision data [8], the search reported in this paper achieves better sensitivity in part by including the entire dataset collected by the ATLAS experiment during Run 2. In addition to the four times larger dataset, the search is further improved by a factor of two via optimising the identification of the hadronic decays of highly boosted W and Z bosons.

2 ATLAS detector

The ATLAS experiment is a multipurpose detector [13] having a forward-backward symmetric cylindrical geometry and almost 4π coverage in solid angle. The inner tracking detectors are immersed in a 2 T magnetic field produced by a thin superconducting solenoid. The tracking detectors cover a pseudorapidity[1] range $|\eta| < 2.5$ using a combination of silicon pixel detectors closest to the beam pipe, followed by silicon microstrip trackers and an outer transition radiation tracker. The innermost layer, known as the insertable B-layer [14, 15], provides high-resolution hits at small radius to improve the tracking performance.

The inner tracking detectors are surrounded by calorimeters and a muon spectrometer. The electromagnetic (EM) calorimeter is a lead/liquid-argon (LAr) sampling calorimeter with high granularity. Its barrel ($|\eta| < 1.475$) and endcap ($1.375 < |\eta| < 3.2$) components provide EM energy measurements of electrons and photons up to a pseudorapidity $|\eta| = 3.2$. In the range used for precision measurements of electrons and photons ($|\eta| < 2.5$ excluding a transition region $1.37 < |\eta| < 1.52$), the EM calorimeter is segmented into three layers along the shower depth, providing excellent measurements of photon properties and allow-

[1] ATLAS uses a right-handed coordinate system with its origin at the nominal interaction point (IP) in the centre of the detector and the z-axis along the beam pipe. The x-axis points from the IP to the centre of the LHC ring, and the y-axis points upward. Cylindrical coordinates (r, ϕ) are used in the transverse plane, ϕ being the azimuthal angle around the z-axis. The pseudorapidity is defined in terms of the polar angle θ as $\eta = -\ln\tan(\theta/2)$.

JHEP07(2023)125

ing precise photon identification. A steel/scintillator-tile hadronic calorimeter covers the central pseudorapidity range $|\eta| < 1.7$. The endcap and forward regions are instrumented up to $|\eta| = 4.9$ with LAr calorimeters for EM and hadronic energy measurements.

The muon spectrometer (MS) comprises separate trigger and high-precision tracking chambers measuring the deflection of muons in a magnetic field generated by superconducting air-core toroidal magnets. The field integral of the toroids ranges between 2.0 and 6.0 T m across most of the detector. A set of precision chambers covers the region $|\eta| < 2.7$ with three layers of monitored drift tubes, complemented by cathode-strip chambers in the forward region, where the background is highest. The muon trigger system covers the range $|\eta| < 2.4$ with resistive-plate chambers in the barrel, and thin-gap chambers in the endcap regions.

Events are selected from the LHC's pp bunch crossings, which occur at a rate of 40 MHz, by a first-level trigger implemented in custom hardware followed by a software-based high-level trigger that employs algorithms similar to those used in offline event reconstruction [16]. The first-level trigger selects events at a rate of 100 kHz by using a subset of detector information, with the high-level trigger then accepting events for offline analysis at the rate of about 1 kHz. An extensive software suite [17] is used in data simulation, in the reconstruction and analysis of real and simulated data, in detector operation, and in the trigger and data acquisition systems of the experiment.

3 Data collection and Monte Carlo event simulation

3.1 Data samples

The data used for this analysis were collected by the ATLAS detector from 2015 to 2018 when the LHC provided pp collisions at $\sqrt{s} = 13$ TeV. Events were selected using a single-photon trigger with loose photon identification requirements based upon EM calorimeter cluster shower-shape variables [18]. The trigger with a photon transverse energy (E_{T}^{γ}) threshold of 140 GeV is fully efficient for events used in this search. In addition to the trigger selection, events are required to have at least one offline reconstructed signal photon matched to the object that fired the photon trigger. After requiring that all detector systems were recording high-quality data, the final dataset has an integrated luminosity of 139 fb^{-1} [19, 20].

3.2 Monte Carlo simulation

Monte Carlo (MC) event generators were used to simulate SM background events and BSM heavy-boson signal events. These simulated event samples are used to optimize the event selection for the new-BSM-boson search and validate the parameterization of the templates used to fit the $W/Z + \gamma$ mass distributions. The largest background is due to single-photon production in association with jets (γ+jets) where the jet fulfils the boson-tagging criteria used to identity the large-R jets from W/Z boson hadronic decays. These events were simulated using the Sherpa 2.2.2 generator [21], with up to two additional parton emissions included at next-to-leading-order (NLO) precision and up to four additional partons

JHEP07(2023)125

at leading-order (LO) precision. The matrix elements of these events were calculated with the Comix [22] and OpenLoops [23, 24] libraries and then matched to the Sherpa parton shower [25] using the MEPS@NLO prescription [26–29]. The NNPDF3.0nnlo [30] parton distribution function (PDF) set was used to describe the parton distributions in the incoming protons. The irreducible SM background from the hadronic decays of W and Z bosons produced with a radiated photon was simulated at LO precision with the Sherpa 2.1.1 generator, and the parton distributions were modelled with the CT10 PDF set [31]. The SM $t\bar{t}+\gamma$ process was simulated with a matrix element at LO with MadGraph5_aMC@NLO 2.3.3 [32], followed by Pythia 8.186 [33] for the parton showering. The NNPDF2.3lo PDF set [34] and a set of tuned parameters called the A14 tune [35] were used for this $t\bar{t}+\gamma$ event generation.

Various samples of simulated BSM boson signal events are used to optimize the event selection criteria and to estimate the acceptance and efficiency for the detection of the $X^{\pm} \to W^{\pm}\gamma$ and $X^0 \to Z\gamma$ signals. The production of the $X^{\pm}$ and X^0 bosons was modelled in a narrow-width approximation where the natural width of the bosons is much smaller than the expected experimental resolution of the invariant mass of the $W^{\pm}\gamma$ and $Z\gamma$ resonances.

The production of a spin-0 boson decaying into $Z\gamma$ was simulated in gluon-gluon fusion, $gg \to X^0 \to Z\gamma$ [36]. This process was modelled with the MC generator Powheg Box v2 [37] at NLO precision as used for SM $H \to Z\gamma$ production, with the Higgs boson mass varied. The CT10 PDF set was used to generate these events. The parton showering was modelled with Pythia 8.212 [38] with the AZNLO tune [39].

The spin-1 resonance $q\bar{q}' \to X^{\pm} \to W^{\pm}\gamma$ signal process event generation utilized the heavy-vector-triplet framework [3] for event kinematic modelling. The simulations of the spin-2 $gg \to X^0 \to Z\gamma$ and $q\bar{q} \to X^0 \to Z\gamma$ signal events are based on a resonance model benchmarked from the Higgs characterization model framework with s-channel direct couplings between the spin-2 heavy resonance and the SM Z boson and the γ [40–42]. The MadGraph5_aMC@NLO v2.3.3 MC generator was used at LO precision, followed by Pythia 8.212 for the parton showering with the NNPDF2.3lo PDF set and the A14 tune. In these models the W (Z) boson is produced longitudinally (transversely) polarized. In samples with Pythia used for parton showering, decays of c- and b-hadrons were simulated with EvtGen 1.2.0 [43].

The resulting MC event samples were processed using a detailed simulation of the ATLAS detector with Geant4 [44, 45], and then passed through the same reconstruction algorithms as those used for the data. Effects of multiple pp collisions (pile-up) are included during reconstruction by overlaying inelastic events simulated with Pythia 8.186 using the A3 tune [46] and the NNPDF2.3lo PDF set. These minimum-bias events are overlaid with multiplicity distributions that approximately match the pile-up observed in the data. A pile-up reweighting approach is then performed to correct for the residual difference between simulation and data in the analysis.

A summary of the MC generators used for the SM and BSM processes is given in table 1.

JHEP07(2023)125

Process	Matrix element generator	QCD order	PDF	Parton shower
SM backgrounds				
SM γ+jets	Sherpa 2.2.2	NLO	NNPDF3.0nnlo	Sherpa MEPS@NLO
SM $W\gamma$ and $Z\gamma$	Sherpa 2.1.1	LO	CT10	Sherpa MEPS@LO
SM $t\bar{t}+\gamma$	MadGraph5_aMC@NLO 2.3.3	LO	NNPDF2.3lo	Pythia 8.186 + EvtGen 1.2.0
Signals				
Spin-0 $gg \to X^0 \to Z\gamma$	Powheg Box v2	NLO	CT10	Pythia 8.212 + EvtGen 1.2.0
Spin-2 $gg \to X^0 \to Z\gamma$	MadGraph5_aMC@NLO 2.3.3	LO	NNPDF2.3lo	Pythia 8.212 + EvtGen 1.2.0
Spin-2 $q\bar{q} \to X^0 \to Z\gamma$	MadGraph5_aMC@NLO 2.3.3	LO	NNPDF2.3lo	Pythia 8.212 + EvtGen 1.2.0
Spin-1 $q\bar{q}' \to X^\pm \to W^\pm\gamma$	MadGraph5_aMC@NLO 2.3.3	LO	NNPDF2.3lo	Pythia 8.212 + EvtGen 1.2.0

Table 1. Generators used for the simulation of SM backgrounds and BSM signals.

4 Event reconstruction

Events are required to pass a loose identification photon trigger with a transverse energy (E_{T}^{γ}) threshold of 140 GeV. Each of these events is then processed through offline particle reconstruction to identify high-E_{T} photons and to search for jets that pass a W/Z boson tagging requirement. The details of the photon, jet and W/Z boson reconstruction and identification are described in this section, along with the categorization applied to define the signal regions for the $X^{\pm} \to W^{\pm}\gamma$ and $X^0 \to Z\gamma$ BSM boson searches.

4.1 Particle reconstruction

Photon candidates are reconstructed from clusters of energy in the EM calorimeter and classified either as converted photons (those with a reconstructed vertex consistent with a $\gamma \to e^+e^-$ conversion) or as unconverted photons [47]. The photon identification algorithm uses shower shape variables measured from both the fine segmentation of the inner layers of the EM calorimeter and the outer layers of the EM and hadronic calorimeters to suppress background from photons from neutral meson decays in jets. For this analysis, *tight* photons are selected, with a measured photon identification efficiency greater than 90% (95%) for unconverted (converted) photon candidates with $E_{\mathrm{T}}^{\gamma} > 200\,\mathrm{GeV}$ [47].

To further reduce backgrounds from jets, an isolation requirement [47] is imposed on the photons, using the transverse energy ($E_{\mathrm{T}}^{\mathrm{iso}}$) deposited in the EM calorimeter within a cone of size $\Delta R \equiv \sqrt{(\Delta\eta)^2 + (\Delta\phi)^2} = 0.4$ centred on the photon candidate, excluding the photon transverse energy within an area $\Delta\eta \times \Delta\phi = 0.125 \times 0.175$. After corrections for photon energy leakage into the isolation cone and contributions from the underlying event and pile-up interactions, the photon isolation transverse energy $E_{\mathrm{T}}^{\mathrm{iso}}$ is required to be less than $0.022 \times E_{\mathrm{T}}^{\gamma} + 2.45\,\mathrm{GeV}$. For the signal photons passing the reconstruction and identification requirements, the isolation efficiency is approximately 98%. Events selected for analysis must have at least one isolated photon candidate with $E_{\mathrm{T}}^{\gamma} > 200$ GeV and $|\eta^{\gamma}| < 1.37$. The η requirement is motivated by the fact that the photon from a signal event tends to be more central than those from the background.

Jets are reconstructed using charged-particle tracks and calorimeter energy clusters, combining their information to optimize the measurement of the jet direction and energy [48]. The clustering method is that of the anti-k_t algorithm [49, 50] with radius

JHEP07(2023)125

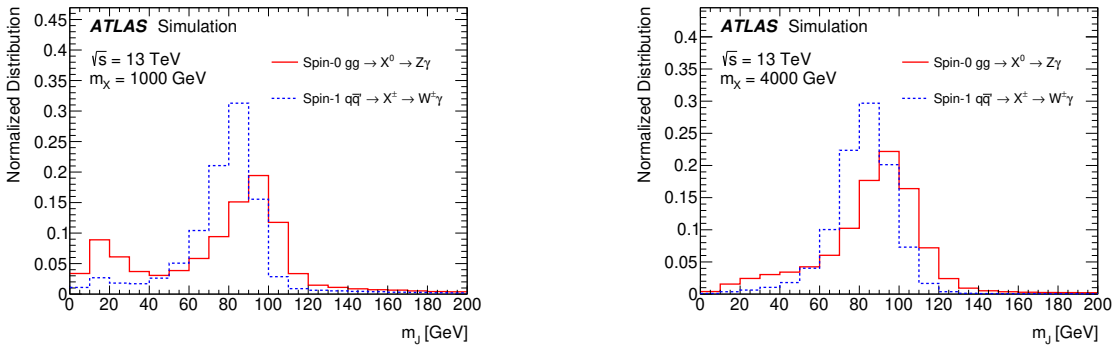

(a) **(b)**

Figure 1. The jet mass distribution of large-R jets originating from the hadronic decay of W and Z bosons produced from the decay of BSM bosons with mass (a) $m_X = 1000\,\text{GeV}$ and (b) $m_X = 4000\,\text{GeV}$. The decays simulated are for the production models $q\bar{q}' \to X^{\pm} \to W^{\pm}\gamma$ with a spin-1 resonance $X^{\pm}$ and $gg \to X^0 \to Z\gamma$ with a spin-0 resonance X^0. The Z bosons from $Z\gamma$ decays of spin-2 resonances have jet mass distributions very similar to those shown for spin-0 resonances.

parameter $R = 1.0$. In order to reduce contributions to the jet from pile-up, a trimming algorithm [51] is applied, which removes contributions from sub-jets clustered using the k_t algorithm [52] with $R = 0.2$ if they carry less than 5% of the jet's transverse momentum. The jets are calibrated to the level of stable final-state particles using MC simulations [53]. Jets are selected if they have a transverse momentum $p_{\text{T}}^J > 200\,\text{GeV}$ and are within a pseudorapidity region $|\eta^J| < 2.0$, where the inner tracker has good charged-particle tracking coverage. The jets are also required to be separated from photons by $\Delta R(J, \gamma) > 1.0$.

A W or Z boson produced by the decay of a boson with a mass of the order of a few TeV is highly boosted, with the di-quark decay products often forming a single large-R jet. The characteristics of these di-quark jets can be used to distinguish W/Z bosons from a large background of jets originating from single quarks or gluons. The main distinguishing features are the jet mass and the presence of two-prong substructure within the jet.

The jet mass (m_J) is calculated using a combination of particle four-momenta measured from charged-particle tracks and calorimeter cell energies [54]. The jet mass resolution ranges from 8% to 15% for jets with transverse momentum between 500 and 2500 GeV, respectively. Reconstructed jet mass distributions from simulated hadronic decays of W and Z bosons are shown in figure 1. The low mass tail is caused by events where the decay products from a W or Z boson are not fully captured in the large-R jet. The effects are different for Z and W bosons since the Z boson from X^0 decay is transversely polarized whereas the W boson from $X^{\pm}$ decay is longitudinally polarized. The jet mass is required to be in a window around the boson mass where the window's size is optimized as a function of p_{T}^J to maximize the significance of the W or Z boson selection over multijet backgrounds [55]. The size of the mass window increases from about 20 to 50 GeV as p_{T}^J increases from 500 to 2500 GeV. For a large-R jet with $p_{\text{T}} < 500\,\text{GeV}$ ($p_{\text{T}} > 2500\,\text{GeV}$), the criterion defined at $p_{\text{T}} = 500\,\text{GeV}$ ($p_{\text{T}} = 2500\,\text{GeV}$) is applied.

JHEP07(2023)125

The two-prong jet substructure from hadronic W/Z boson decays is identified using the energies and pairwise angular distances between clusters of particles within the large-R jets. This is quantified with a variable D_2 defined as the ratio $\epsilon_3/[\epsilon_2]^3$ of N-point energy correlation functions ϵ_N computed from the jet constituents [56, 57]. This variable exploits the sensitivity of ϵ_2 to the hadronic shower produced from a single quark or gluon versus ϵ_3, which is sensitive to the two hadronic-jet clusters produced from the di-quark decay of W/Z bosons. Studies using simulations and data were used to choose the requirements on D_2 that optimize the W/Z boson identification significance [55]. The chosen upper limit on D_2 varies from 1.0 at low jet p_{T} to slightly above 2.0 at high jet p_{T} for the W/Z hadronic jets used in this analysis.

For the fraction of Z bosons that decay into $b\bar{b}$, the purity of the selection can be further improved by applying b-hadron identification requirements. A tagging algorithm is used that exploits the long lifetime of b-hadrons, which leads to tracks with large impact parameters and to secondary vertices. The outputs of three b-tagging techniques are combined into a single multivariate discriminant, called MV2c10, allowing the selection of b-hadrons with various efficiencies and background rejections [58]. This b-tagging algorithm is applied to variable-radius (VR) track-jets associated with the large-R jet, as determined by the ghost-association algorithm [59]. The VR track-jets are reconstructed from ID tracks using the anti-k_t algorithm with a variable radius parameter R that ranges between 0.02 and 0.4 depending on the jet p_{T} [60]. The tagging efficiency is determined with simulated $t\bar{t}$ events and corrected to the measurement in data [61]. A working point with a b-tagging efficiency of 70% is used. Two VR track-jets are required to pass this b-tagging requirement to select $Z \to b\bar{b}$ events.

4.2 Event selection and categorization

The events selected are required to have a photon with $E_{\mathrm{T}}^{\gamma} > 200\,\mathrm{GeV}$ and $|\eta^{\gamma}| < 1.37$ and a jet with $p_{\mathrm{T}}^{J} > 200\,\mathrm{GeV}$ and $|\eta^{J}| < 2.0$, using the identification criteria described above. These selection criteria are called the "baseline selection" for this analysis. The pp interaction vertex selected for reconstruction of these physics objects is the one with the highest sum of the p_{T}^2 of the tracks coming from the vertex. If multiple photons or jets satisfy the photon/jet selection criteria, those with the highest transverse energy or momentum are used. The search considers resonances with masses larger than 1 TeV. Below this mass, the signal selection efficiency drops significantly because of the criteria used to select the hadronic decays of the W/Z bosons, and searches for $pp \to X \to W/Z+\gamma$ with leptonic W/Z boson decays are more sensitive. The search range is limited to 6.8 TeV using the highest-mass γ+jet event observed in data. The selected events are further sorted into exclusive categories of different W and Z boson identification purities to maximize the signal sensitivity.

For the $X^{\pm} \to W^{\pm}\gamma$ search, two categories are defined according to the D_2 and jet mass criteria shown below, with the category designation indicated in parentheses.

- *pass* D_2 and W boson mass selection (D2),
- *fail* D_2 and *pass* W boson mass selection (WMASS).

JHEP07(2023)125

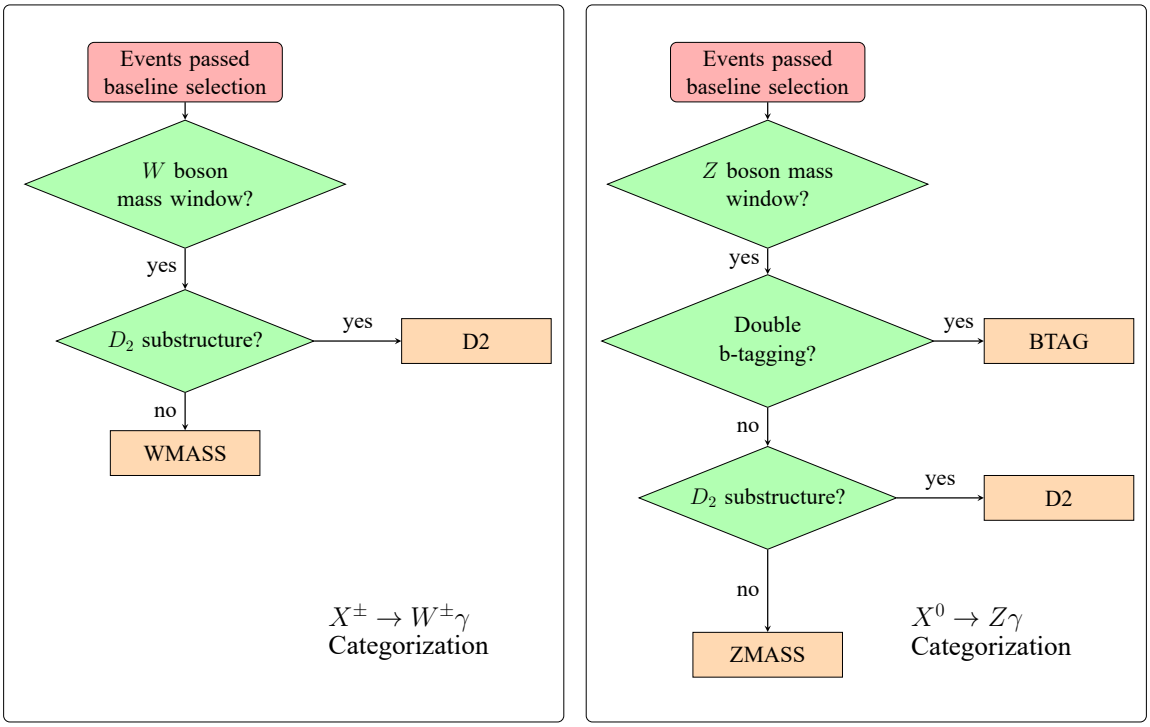

Figure 2. The flow charts of event categorization of $X^{\pm} \to W^{\pm}\gamma$ and $X^0 \to Z\gamma$.

For the $X^0 \to Z\gamma$ search, three categories are defined, based on the b-tagging, D_2 and jet mass criteria shown below.

- *pass* two b-tagged sub-jets and *pass* Z boson mass selection (BTAG),
- *fail* two b-tagged sub-jets: *pass* D_2 and Z boson mass selection (D2),
- *fail* two b-tagged sub-jets: *fail* D_2 and *pass* Z boson mass selection (ZMASS).

Figure 2 illustrates the categorization of $X^{\pm} \to W^{\pm}\gamma$ and $X^0 \to Z\gamma$ events.

The rejection of the dominant γ+jet background varies strongly among the categories, being highest in those using jet substructure and mass information. A further optimization of the signal sensitivity is implemented by varying the photon E_{T}^{γ} threshold as a function of the invariant mass $m_{J\gamma}$ of the photon and large-R jet, where the figure of merit is the statistical-only significance of the simulated BSM signal over the expected SM backgrounds, where the SM backgrounds are estimated from the simulated background samples described in section 3.2. This photon E_{T}^{γ} optimization is done separately for each of the event categories, taking advantage of the large difference in photon and jet kinematics between signal and background. The photon E_{T}^{γ} threshold increases with $m_{J\gamma}$, varying from about 300 to 1200 GeV. This results in a small loss of signal efficiency, but a very large suppression of the SM backgrounds. Figure 3 shows the total signal selection efficiencies after optimization of the photon E_{T}^{γ} thresholds, and also the contributions to the signal selection from each of the individual categories. The BTAG category has the lowest efficiency but the highest signal purity. The spin-2 $Z\gamma$ channel with gg production mode

JHEP07(2023)125

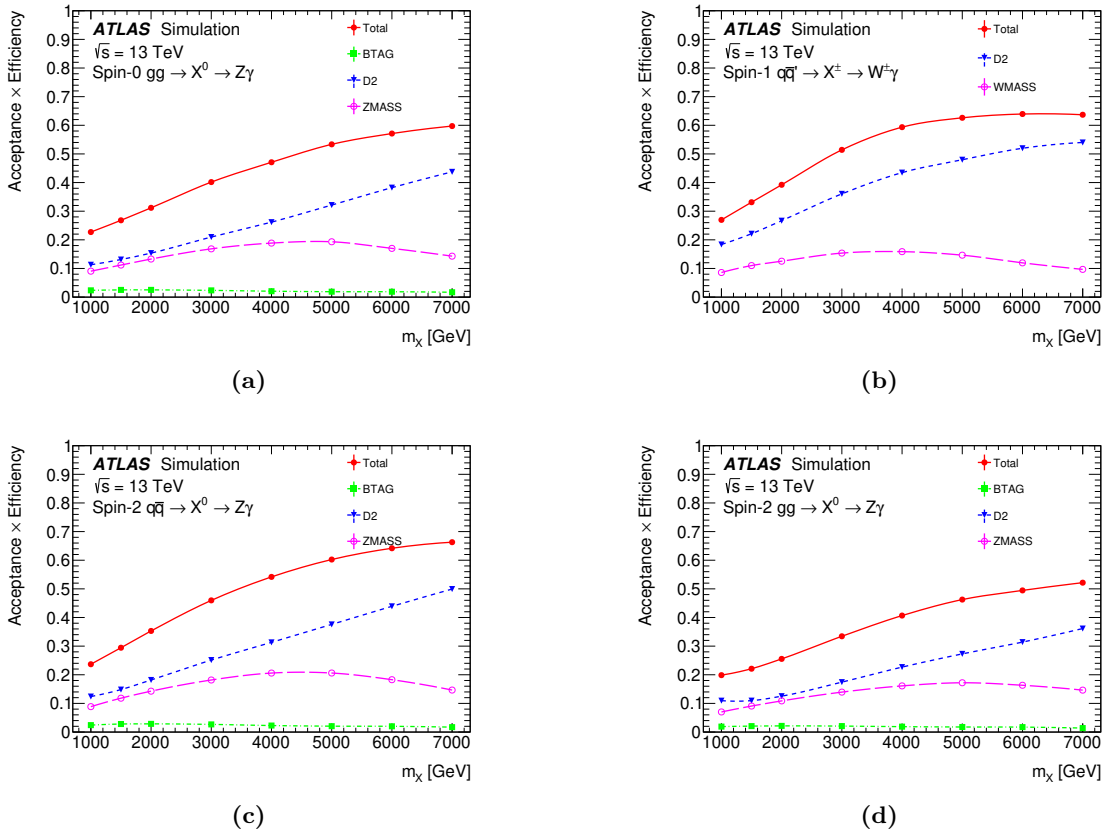

Figure 3. Total efficiencies for the selection of signal events after categorization and application of the tighter photon E_{T}^{γ} selection used to optimize the signal significance: (a) spin-0 $gg \to X^0 \to Z\gamma$, (b) spin-1 $q\bar{q}' \to X^{\pm} \to W^{\pm}\gamma$, (c) spin-2 $q\bar{q} \to X^0 \to Z\gamma$, and (d) spin-2 $gg \to X^0 \to Z\gamma$. In addition to the total efficiency, contributions to the signal selection from each of the separate event categories are shown. The efficiencies calculated from MC samples with W/Z hadronic decays are shown as the points on each curve. The line presents interpolated results.

has a different X boson polarization than the $q\bar{q}$ production mode, leading to a longer lower tail in the photon and jet p_{T} distributions, and wider pseudorapidity distributions, and therefore a lower baseline selection efficiency. For signals with a resonance mass above 4 TeV, the applied D_2 requirement is relatively loose, which results in most signal events entering the D2 category and the W/ZMASS selection appearing to lose efficiency. The signal selection efficiencies increase with the mass m_X, ranging from about 20% at the lowest mass to about 60% at 6.8 TeV.

5 Signal and background modelling

The search for BSM boson signals is carried out by inspecting the invariant mass distribution of the highest-E_{T} photon and large-R jet identified in each event. The distribution of $m_{J\gamma}$ from SM backgrounds falls smoothly over the mass range 1.0 to 6.8 TeV used in this search. The presence of a boson $X^{\pm} \to W^{\pm}\gamma$ or $X^0 \to Z\gamma$ would therefore appear in the

JHEP07(2023)125

data as an excess of events above the background $m_{J\gamma}$ distribution in a relatively narrow mass region around m_X. The search sensitivity is quantified by fitting the data with the sum of the SM background plus a signal that is parameterized from simulations of the various production modes described in section 3.2. The functional forms chosen for the background and signal are described below, and the fitting procedure used to search for signals is presented in section 7.

5.1 SM background modelling

The SM background is dominated by γ+jet events. In the D2 (W/ZMASS) event category, the production of a photon in association with light-flavour jets and c-jets contributes about 92% (96%) of the SM background, while in the BTAG category the contribution from SM γ+b-jet events is about 88%. The next highest background contribution comes from SM $W\gamma$ and $Z\gamma$ production with the W/Z bosons decaying hadronically. The contribution from SM $t\bar{t}$+γ production is found to be negligible compared to other SM backgrounds after the final event selection. Contributions from events with photons misidentified as jets are found to be small and not significant in changing the background shape from the dominant γ+jet backgrounds.

The $m_{J\gamma}$ distribution of the background is parameterized with a function that is flexible enough to accommodate the background shape in each of the four event categories used in the signal search. The function chosen to model the background is taken from ref. [62], and is described by eq. (5.1):

$$\mathcal{B}(m_{J\gamma};\boldsymbol{p}) = (1-x)^{p_1} x^{p_2+p_3\log(x)}, \tag{5.1}$$

where $x = m_{J\gamma}/\sqrt{s}$, and $\boldsymbol{p}$= (p_1, p_2, p_3) is a vector of parameters used to control the shape of the distribution. The ability of the function to describe backgrounds is tested using $m_{J\gamma}$ distributions from MC simulations which have about five times the number of data events in the signal region. The number of parameters p_i is determined by testing the ability of each function to fit these background $m_{J\gamma}$ distributions over the mass range used for each category. The determination of the number of parameters also includes studies of fits of the background-only mass distributions to a signal-plus-background hypothesis in order to quantify any "spurious signal" (N^{SS}) resulting from the parameterization with the procedure documented in ref. [63]. The number of fit parameters that minimizes the spurious signal is chosen. With this criterion, the number of fit parameters is two or three depending on the category and signal model. The spurious signal is then included as a systematic uncertainty in the fitted signal yield associated with the background fit function, and included in the statistical treatment used for the signal search. The choice of functional form and the spurious signal obtained from MC simulated samples are validated with data in a control region. The control region (CR) events are selected with the photon required to be in the forward pseudorapidity region $1.52 < |\eta^{\gamma}| < 2.37$. This CR is found to have a small signal leakage which varies from 2% to 17% depending on the signal type and the resonance mass. This validation process confirms that the chosen functional form is flexible enough to model the $m_{J\gamma}$ distribution in data.

JHEP07(2023)125

5.2 BSM signal modelling

The distribution of $m_{J\gamma}$ for a given BSM boson mass is generated with a natural width that is much smaller than the experimental resolution. These MC events are passed through a full detector simulation and selected in the same way as data events. The signal $m_{J\gamma}$ distribution is modelled with a double-sided Crystal Ball (DSCB) function [64]. This function is found to be the best model to describe the peak and the long tails of the signal distribution. It is described by eq. (5.2):

$$\begin{aligned}
&\mathcal{S}(m_{J\gamma};N,\mu,\sigma,\alpha_1,n_1,\alpha_2,n_2) \\
&= N\cdot\begin{cases}
\left(\frac{n_1}{|\alpha_1|}\right)^{n_1}\exp\left(-\frac{|\alpha_1|^2}{2}\right)\left(\frac{n_1}{|\alpha_1|}-|\alpha_1|-\frac{m_{J\gamma}-\mu}{\sigma}\right)^{-n_1} & \frac{m_{J\gamma}-\mu}{\sigma}\leq-\alpha_1 \\
\exp\left(-\frac{(m_{J\gamma}-\mu)^2}{2\sigma^2}\right) & -\alpha_1<\frac{m_{J\gamma}-\mu}{\sigma}\leq\alpha_2 \\
\left(\frac{n_2}{|\alpha_2|}\right)^{n_2}\exp\left(-\frac{|\alpha_2|^2}{2}\right)\left(\frac{n_2}{|\alpha_2|}-|\alpha_2|+\frac{m_{J\gamma}-\mu}{\sigma}\right)^{-n_2} & \alpha_2<\frac{m_{J\gamma}-\mu}{\sigma}.
\end{cases}
\end{aligned} \tag{5.2}$$

The DSCB function includes a central Gaussian core, to model the experimental resolution of the signal, with tails parameterized with power-law functions above and below the peak. The Gaussian core has a mean μ and width σ, while the low (high) $m_{J\gamma}$ tail is fitted using the parameters α_1 (α_2) and n_1 (n_2), with all the parameters constrained to be positive in the fit.

This signal model is used to fit the $m_{J\gamma}$ distribution generated from the four signal hypotheses at masses ranging from 1.0 to 7.0 TeV in steps of 1.0 TeV, with one additional mass point at 1.5 TeV. A linear interpolation between adjacent mass points is performed for each of the fit parameters to obtain the signal shapes at intermediate mass values. The width of the central core grows linearly from a σ of about 30 to 120 GeV as the boson mass increases from 1.0 to 7.0 TeV.

6 Systematic uncertainties

The systematic uncertainties considered in this analysis come from the background estimation, the signal prediction and the detector performance. The effects of these systematic uncertainties are parameterized according to their impact on the signal efficiency, the signal shape peak position and the core width of the signal shape. All these uncertainties are included in the statistical procedure when fitting the signal-plus-background model to the data.

The potential bias from the background fit function describing the data $m_{J\gamma}$ distribution is evaluated using the spurious-signal test described in section 5. A spurious signal is treated as a systematic uncertainty arising from the choice of background parameterization and only affects the signal yield during the fitting procedure. Assuming there is no signal in the data, the impact of spurious-signal uncertainties when setting cross-section limits decreases from 20% to a negligible value with increasing resonance mass.

The uncertainty in the luminosity determination affects the signal yield prediction. The integrated luminosity is measured using the LUCID-2 Cherenkov detector [65] and calibrated with a van der Meer scan following the methodology documented in ref. [66].

JHEP07(2023)125

This results in a 1.7% uncertainty in the 139 fb^{-1} integrated luminosity collected during the 2015–2018 data-taking period.

The uncertainty in the modelling of inelastic pp pile-up collisions overlaid on the simulation introduces a 2% uncertainty in the signal detection efficiency.

The uncertainty in the photon energy measurement affects the signal selection efficiency and the shape of the invariant mass $m_{J\gamma}$ distribution. The photon energy is calibrated using the method described in ref. [47]. Various sources of uncertainty contribute to the measurement of the photon energy scale and the photon energy resolution. The photon identification, isolation and trigger efficiencies are all measured from data following the method in refs. [18, 47].

The uncertainty in large-R jet energy and mass calibration also affects the signal selection efficiency and the $m_{J\gamma}$ shape. The large-R jet energy and mass are calibrated with the method described in ref. [53]. The impact of the jet energy resolution uncertainty is estimated by applying Gaussian smearing to each jet so as to degrade the jet p_{T} resolution by 2% [53]. To estimate the impact of the jet mass resolution (JMR) uncertainty, a similar method is used to degrade the JMR by 20%. Similarly, the effect of uncertainty in the D_2 resolution is estimated by degrading the D_2 resolution by 15% with Gaussian smearing.

The uncertainty in the jet-flavour tagging efficiency measurement impacts both the signal selection efficiency and the $m_{J\gamma}$ distribution. The jet-flavour tagging efficiency is measured in a data region enriched in $t\bar{t}$ events and compared with simulations to derive corrections [61]. The uncertainties for high-p_{T} VR track-jets are extrapolated with simulated samples because there are too few events in data [67]. The associated uncertainties are grouped into b-jet, c-jet and light-flavour jet components that are described by uncorrelated eigenvector variations.

The uncertainty in the signal selection efficiency due to the PDF set is evaluated using the eigenvector variations following the method in ref. [68]. The uncertainty in the signal selection efficiency from the QCD scales is estimated from alternative samples with the renormalization scale (μ_{r}) and factorization scale (μ_{f}) varied by factors of 0.5 and 2 with the cases that differ by a factor of four being ignored. The uncertainty in the signal selection efficiency from the parton shower is estimated from alternative Pythia samples with different values of the A14 tune parameters, affecting the underlying events, initial/final-state radiation, multiple parton interactions and colour reconnection [35].

The limited size of the generated signal samples introduces a systematic uncertainty in the signal parameterization with analytic functions as described in section 5.2. Only the effect on the signal resolution is found to have a significant impact on the final result and is included in the statistical analysis as a systematic uncertainty.

Table 2 summarizes the main sources of signal uncertainty and their impact on the signal measurement. The dominant uncertainties for the signal in this analysis come from jet mass scale, jet mass resolution and jet energy resolution.

JHEP07(2023)125

Source of uncertainty	Impact on signal yield [%]
Luminosity	1.7
Jet energy scale	1–7
Jet mass scale	1–20
Jet mass resolution	2–12
Jet D_2 resolution	2
Photon energy scale	0.2
Photon energy resolution	0.1
Flavour tagging	1–8
Pile-up	0–3
PDF	2–12
QCD	2
Parton shower	1–2
	Impact on signal peak position [%]
Jet energy scale	0–4
Jet mass scale	0–1
Photon energy scale	0.4
	Impact on signal resolution [%]
Jet energy scale	1–7
Jet mass scale	0–11
Jet energy resolution	5–20
Photon energy scale	0.2–2
Photon energy resolution	0.2–1.2
Flavour tagging	0.2–4
Signal sample statistics	1–6

Table 2. The impact of systematic uncertainties on the signal yield, signal peak position and signal peak resolution. Presented numbers are derived before performing the statistical analysis. A range of values shows the variation of the uncertainty across the m_X range.

7 Statistical analysis

The search for BSM resonance signals above a smoothly falling background $m_{J\gamma}$ mass distribution is carried out with a statistical procedure based on an unbinned likelihood fit over the $m_{J\gamma}$ spectrum, implemented in a `RooFit` [69] and `RooStats` [70] framework. The likelihood function is defined as the product of several factors using a Poisson model for the observed event yield in each category. This product includes probabilities for events distributed in $m_{J\gamma}$ as described by a model based on the sum of signal ($\mathcal{S}$) and background

JHEP07(2023)125

($\mathcal{B}$) probability density functions described in section 5 and probabilities for auxiliary measurements with their prior distributions ($\mathcal{G}$). This can be written as:

$$\begin{aligned}\mathcal{L}(\boldsymbol{m}_{J_\gamma}^{\text{obs}}|\,\sigma_{\text{had}},\boldsymbol{\theta},\boldsymbol{\theta}^{\text{SS}},\boldsymbol{N}^{\text{B}},\boldsymbol{p}) = \prod_{c\in\mathbb{C}}\Bigg\{&\text{Pois}(N_c^{\text{obs}}|N_c^{\text{S}}(\sigma_{\text{had}},\boldsymbol{\theta})+N_c^{\text{SS}}(\theta_c^{\text{SS}})+N_c^{\text{B}})\\ &\times\prod_{i=1}^{N_c^{\text{obs}}}\Bigg[\left(\frac{N_c^{\text{S}}(\sigma_{\text{had}},\boldsymbol{\theta})+N_c^{\text{SS}}(\theta_c^{\text{SS}})}{N_c^{\text{S}}(\sigma_{\text{had}},\boldsymbol{\theta})+N_c^{\text{SS}}(\theta_c^{\text{SS}})+N_c^{\text{B}}}\right)\mathcal{S}(m_{J_\gamma}^{c,i,\text{obs}}|\,\boldsymbol{\theta})\\ &+\left(\frac{N_c^{\text{B}}}{N_c^{\text{S}}(\sigma_{\text{had}},\boldsymbol{\theta})+N_c^{\text{SS}}(\theta_c^{\text{SS}})+N_c^{\text{B}}}\right)\mathcal{B}(m_{J_\gamma}^{c,i,\text{obs}}|\,\boldsymbol{p}^c)\Bigg]\Bigg\}\\ &\times\prod_{s\in\mathbb{S}}\mathcal{G}(0|\theta_s,1)\prod_{c\in\mathbb{C}}\mathcal{G}(0|\theta_c^{\text{SS}},1),\end{aligned}\tag{7.1}$$

where $\boldsymbol{m}_{J_\gamma}^{\text{obs}} = \{m_{J_\gamma}^{1,1,\text{obs}},\cdots,m_{J_\gamma}^{c,i,\text{obs}},\cdots\}$ is a set of observations of $m_{J\gamma}$ in data, c is the label of the various event categories and i the index of events in each category. The Poisson term for each category, $\text{Pois}(N_c^{\text{obs}}|N_c^{\text{S}}(\sigma_{\text{had}},\boldsymbol{\theta})+N_c^{\text{SS}}+N_c^{\text{B}})$, is defined according to observed data events in the signal region, N_c^{obs}, and the expected signal-plus-background yield, which is a sum of the signal yield $N_c^{\text{S}}(\sigma_{\text{had}},\boldsymbol{\theta})$, the background yield N_c^{B}, and the spurious signal N_c^{SS}. The signal yield N_c^{S} can be expanded as a function of the signal production cross-section σ_{had}, which is the parameter of interest (POI) in the statistical analysis. This cross-section σ_{had}, as the abbreviation for $\sigma(pp\to X\to W/Z(\to\text{hadrons})+\gamma)$, includes the production cross-section $\sigma(pp\to X)$ of the resonance and the branching fractions of $X\to W/Z+\gamma$ and $W/Z\to$ hadrons. The experimental and theoretical uncertainties are described by the nuisance parameters (NPs) θ_s for each systematic uncertainty s and shared among categories. A collection of such nuisance parameters is written as $\boldsymbol{\theta}$. These nuisance parameters are constrained with a normal distribution $\mathcal{G}(0|\theta_s,1)$. The spurious-signal contribution N_c^{SS} is formalized as a function of the associated nuisance parameter θ_c^{SS} for each category individually, with this NP following a normal distribution $\mathcal{G}(0|\theta_c^{\text{SS}},1)$. The collection of spurious-signal nuisance parameters is written as $\boldsymbol{\theta}^{\text{SS}}$. Both θ_s and θ_c^{SS} can have an impact on the signal expectation ($N_c^{\text{S}}+N_c^{\text{SS}}$) of the fit model, while the parameter θ_s can also modify the signal shape. The background shape parameters $\boldsymbol{p}^c=(p_1^c,p_2^c,p_3^c)$ are allowed to float during the fit to data and are uncorrelated among categories. The signal model $\mathcal{S}$ is fixed for each tested m_X using the coefficients presented in section 5.

Both the signal and background yields are extracted by maximizing the likelihood as defined in eq. (7.1) for various hypothetical values of m_X. The fit stability is checked with signal injection tests, and no significant bias is observed. For each of these mass points, the p-value of the background-only hypothesis is calculated to test the compatibility of the background-only hypothesis and the data. This is done with the profiled likelihood ratio (PLR) test statistic [71], which is defined as the ratio of the conditional maximum-likelihood value for a POI value of zero to the global maximum-likelihood value. Its distribution in the low resonance mass region ($m_X<4000\,\text{GeV}$) is derived following the asymptotic approach as described in ref. [71]. In the high resonance mass region ($m_X\geq 4000\,\text{GeV}$), test statistic distributions are obtained with the pseudo-experiment sampling method. The

JHEP07(2023)125

Channel	BTAG	D2	VMASS
Spin-0 $gg \to X^0 \to Z\gamma$	436	5 659	20 728
Spin-2 $gg \to X^0 \to Z\gamma$	436	10 772	32 281
Spin-2 $q\bar{q} \to X^0 \to Z\gamma$	436	5 618	18 264
Spin-1 $q\bar{q}' \to X^{\pm} \to W^{\pm}\gamma$	—	6 373	25 146

Table 3. Data yields in various categories defined for the four search channels.

p-value reflects the possibility of background to produce a signal-like excess larger than that found in the fit to the data, which is reported as the significance according to the normal distribution. Beside the significance, an exclusion of the signal model is derived and presented as the 95% confidence level (CL) upper limit on the resonance production cross-section times branching fraction of $X \to W/Z + \gamma$ for hadronic decay of the W/Z bosons. Similar to the p-value, the upper limit is also calculated from PLR distributions but with a running POI value to indicate various signal cross-section hypotheses. The CL_s approach [72, 73] is used for the limit calculation. The limits are calculated in the low resonance mass regions at 20 GeV steps and are based on the asymptotic approach. In the high resonance mass region, limits are derived by using the pseudo-experiment sampling method. To obtain smooth expected limit bands, the expected limits and the corresponding bands are calculated at 500 GeV steps in the high resonance mass region while the observed ones are obtained at 100 GeV steps. Upper limits on $\sigma(pp \to X) \times B(X \to W/Z + \gamma)$ are derived by assuming the branching fractions of W and Z bosons to hadrons to be 67.41% [74] and 69.91% [74] respectively.

8 Results

Table 3 presents the observed number of events in different categories after the final event selection. The yields quoted are for $m_{J\gamma} \geq 800$ GeV in the BTAG and D2 categories and for $m_{J\gamma} \geq 1000$ GeV in the VMASS (ZMASS or WMASS) categories. The BTAG categories are defined in the same way for the three Z signal hypotheses, while for the D2 and VMASS categories the selection criteria for the photon and jet are chosen differently for each channel. The latter optimizes the signal significance by exploiting differences in the $W/Z + \gamma$ production angular distributions and in the decays of the longitudinally polarized W bosons and transversely polarized Z bosons.

The $m_{J\gamma}$ distributions in different categories are shown in figures 4–7 for the four signal channels. The background-only fit result is shown as the solid curve overlaid with a shaded band corresponding to statistical uncertainties in background parameters. Various signal mass hypotheses are also plotted, where the signal cross-sections correspond to the expected upper limits obtained in this analysis. For the BTAG category, the fit range is limited to below 3200 GeV due to the significant loss of sensitivity because of the decrease in b-tagging efficiency beyond that range, while for other categories the fit upper boundary is 7000 GeV. The bottom panel presents the binned local significance (filled bars) from a comparison

JHEP07(2023)125

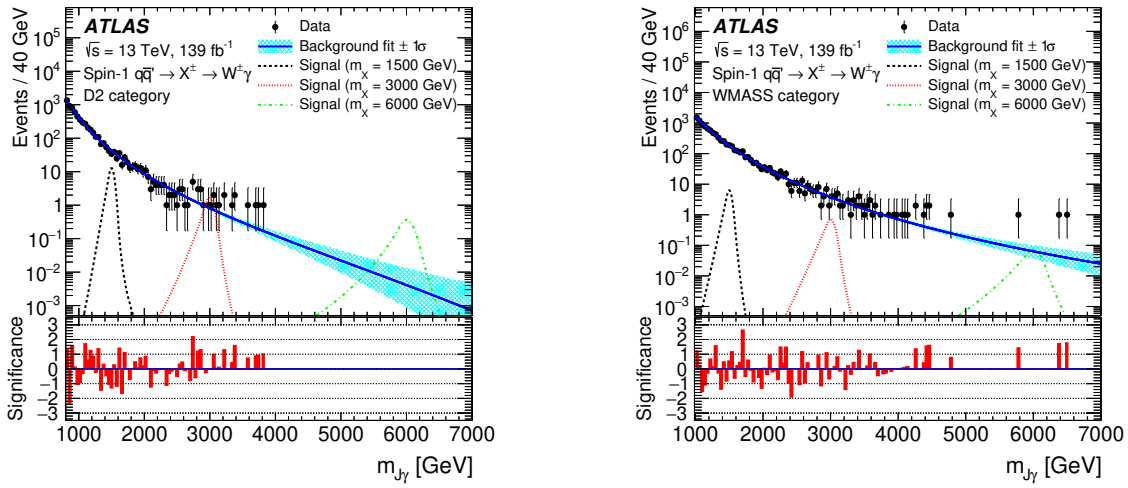

Figure 4. The $m_{J\gamma}$ distributions of data events selected for the spin-1 $q\bar{q}' \to X^{\pm} \to W^{\pm}\gamma$ search in the (a) D2 and (b) WMASS categories. The background-only fit function shape is shown as the solid curve overlaid with a shaded band corresponding to statistical uncertainties in background parameters. Various signal shapes with cross-sections corresponding to expected limits are shown as dashed lines. The bottom panel presents the binned local significance (filled bars) from a comparison of the data with the background fit using a Poisson model [75].

of the data with the background fit using a Poisson model [75]. The background-only model fits the data well, with most of the deviations of the data from the background-only hypothesis having a local significance below two standard deviations.

Having found no significant deviation of the data from the SM background predictions, upper limits on signal cross-sections are calculated at a 95% confidence level for each of the four search channels. The observed cross-section limits (solid curves) are presented in figure 8, along with the expected limits (dotted curves) obtained by assuming only SM backgrounds. The limits range between approximately 0.05 fb and 10 fb for m_X between 1 and 6.8 TeV. The one- and two-standard-deviation bands around the expected limits cover the observed limits almost everywhere, which is consistent with the observation that the data agree well with the background-only expectations. The largest deviation of the observed cross-section limit above the expectation is 2.5σ for spin-0 $gg \to X^0 \to Z\gamma$ production from gluon-gluon fusion at $m_X = 3640$ GeV.

JHEP07(2023)125

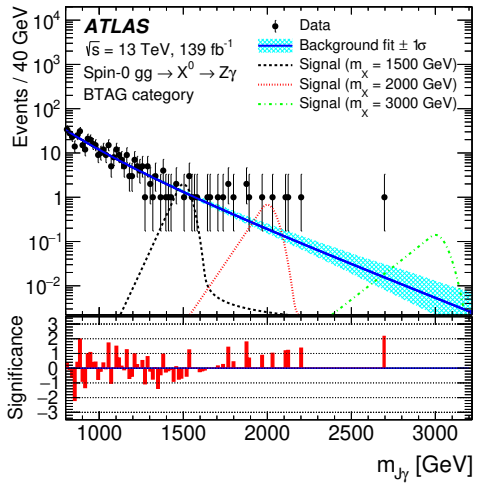

(a)

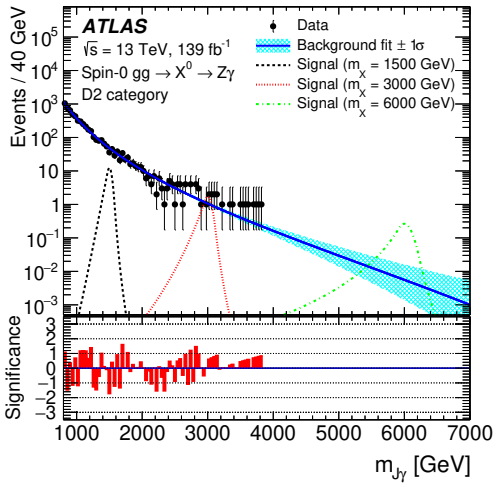

(b)

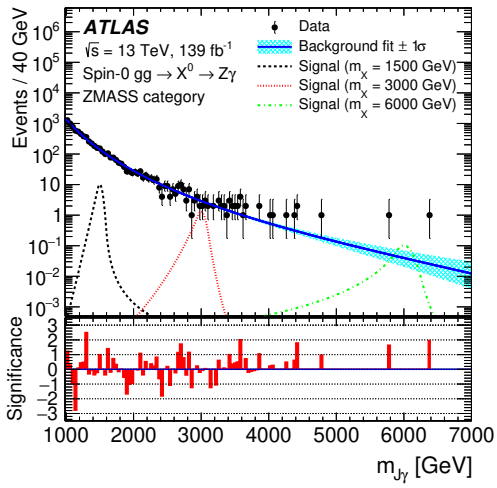

(c)

Figure 5. The $m_{J\gamma}$ distributions of data events selected for the spin-0 $gg \to X^0 \to Z\gamma$ search in the (a) BTAG, (b) D2, and (c) ZMASS categories. The background-only fit function shape is shown as the solid curve overlaid with a shaded band corresponding to statistical uncertainties in background parameters. Various signal shapes with cross-sections corresponding to expected limits are shown as dashed lines. The bottom panel presents the binned local significance (filled bars) from a comparison of the data with the background fit using a Poisson model [75].

JHEP07(2023)125

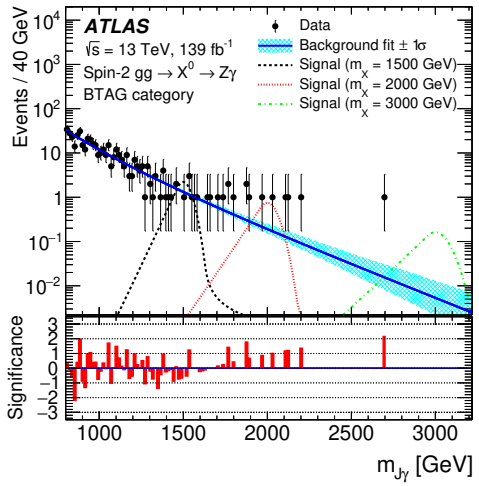

(a)

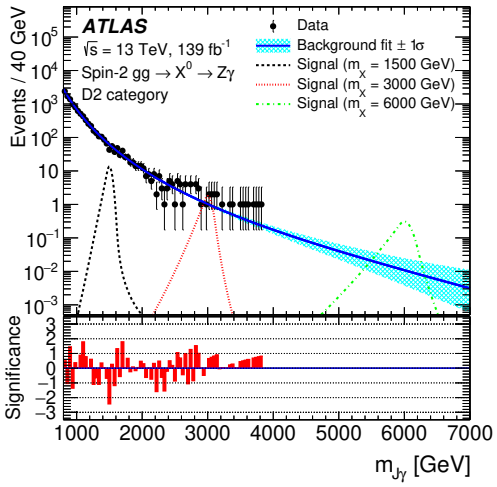

(b)

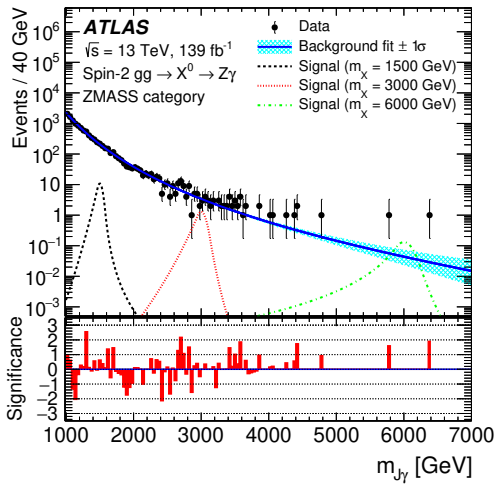

(c)

Figure 6. The $m_{J\gamma}$ distributions of data events selected for the spin-2 $gg \to X^0 \to Z\gamma$ search in the (a) BTAG, (b) D2, and (c) ZMASS categories. The background-only fit function shape is shown as the solid curve overlaid with a shaded band corresponding to statistical uncertainties in background parameters. Various signal shapes with cross-sections corresponding to expected limits are shown as dashed lines. The bottom panel presents the binned local significance (filled bars) from a comparison of the data with the background fit using a Poisson model [75].

JHEP07(2023)125

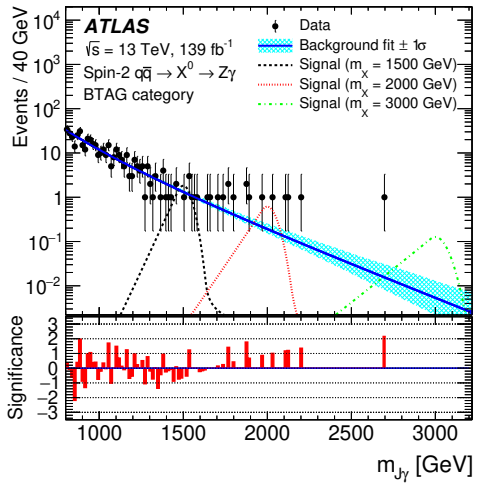

(a)

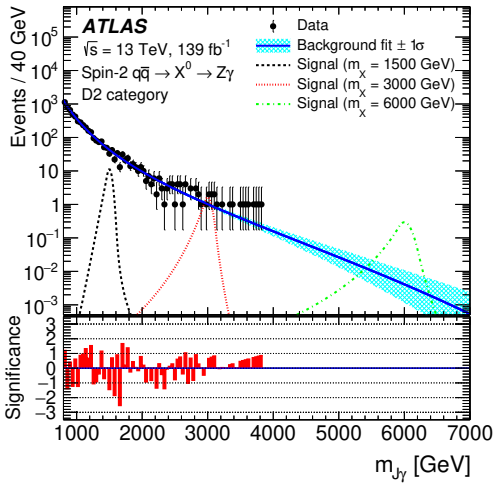

(b)

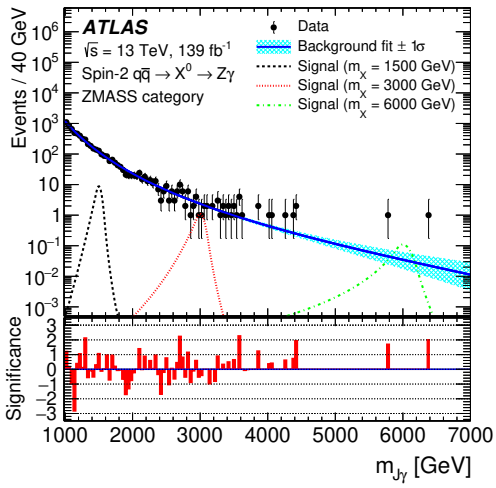

(c)

Figure 7. The $m_{J\gamma}$ distributions of data events selected for the spin-2 $q\bar{q} \to X^0 \to Z\gamma$ search in the (a) BTAG, (b) D2, and (c) ZMASS categories. The background-only fit function shape is shown as the solid curve overlaid with a shaded band corresponding to statistical uncertainties in background parameters. Various signal shapes with cross-sections corresponding to expected limits obtained in this analysis are shown as dashed lines. The bottom panel presents the binned local significance (filled bars) from a comparison of the data with the background fit using a Poisson model [75].

JHEP07(2023)125

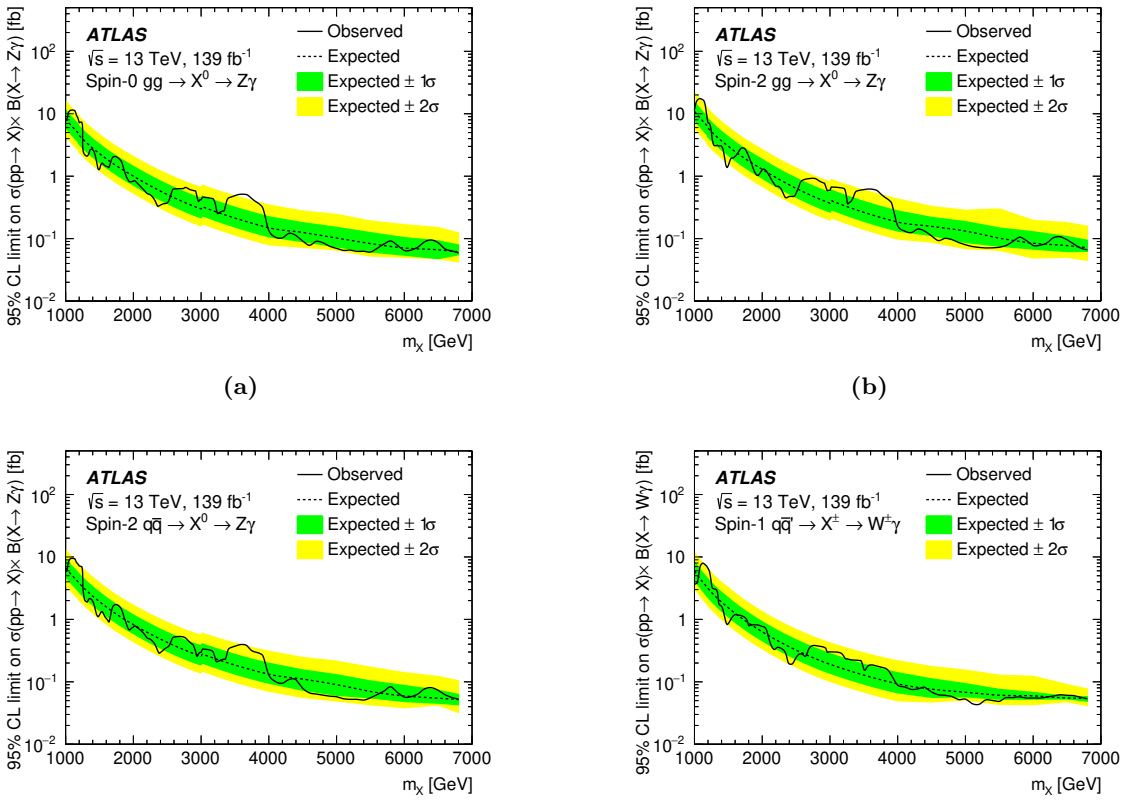

Figure 8. The 95% CL upper limits on $\sigma(pp \to X) \times B(X \to W/Z\gamma)$ as a function of m_X for (a) spin-0 $gg \to X^0 \to Z\gamma$, (b) spin-2 $gg \to X^0 \to Z\gamma$, (c) spin-2 $q\bar{q} \to X^0 \to Z\gamma$ and (d) spin-1 $q\bar{q}' \to X^{\pm} \to W^{\pm}\gamma$. The observed limits are shown as a solid black line and the expected ones are shown as a dashed line with the 1σ (2σ) uncertainty band presented as the green (yellow) band. Small discontinuities in $pp \to X^0 \to Z\gamma$ limits are due to dropping the BTAG category from the limit calculation for mass points with $m_X > 3000\,\text{GeV}$. Limits for $m_X < 4000\,\text{GeV}$ are derived with the asymptotic approach, while the ones for higher masses are calculated with the pseudo-experiment sampling method.

JHEP07(2023)125

9 Conclusion

Results of searches for high-mass bosons decaying to $W\gamma$ and $Z\gamma$ final states are presented, using 139 fb^{-1} of $\sqrt{s} = 13$ TeV pp collision data collected with the ATLAS detector during the operation of the LHC from 2015 to 2018. The analysis maximizes the sensitivity of the search by selecting events passing a high-E_{T} photon trigger and identifying jets from the hadronic decays of highly boosted W and Z bosons. Distributions of the invariant mass of the photon-jet pairs in the mass range from 1.0 to 6.8 TeV are used to search for $X^{\pm} \to W^{\pm}\gamma$ and $X^0 \to Z\gamma$ signals above a smoothly falling SM background. No evidence of a new resonance is found, and 95% confidence-level upper limits on the resonance production cross-section times decay branching fraction are set. These vary from about 10 to 0.05 fb as the heavy-boson mass increases from 1.0 to 6.8 TeV. Individual studies are carried out for resonances with spin 0, 1, and 2 produced via gluon-gluon fusion and $q\bar{q}$ annihilation, currently providing the most stringent exclusion limits for these processes. Due to improved analysis techniques, the search sensitivity at high mass has been improved by a factor of two relative to that expected from the increase in integrated luminosity of the analysed data.

Acknowledgments

We thank CERN for the very successful operation of the LHC, as well as the support staff from our institutions without whom ATLAS could not be operated efficiently.

We acknowledge the support of ANPCyT, Argentina; YerPhI, Armenia; ARC, Australia; BMWFW and FWF, Austria; ANAS, Azerbaijan; CNPq and FAPESP, Brazil; NSERC, NRC and CFI, Canada; CERN; ANID, Chile; CAS, MOST and NSFC, China; Minciencias, Colombia; MEYS CR, Czech Republic; DNRF and DNSRC, Denmark; IN2P3-CNRS and CEA-DRF/IRFU, France; SRNSFG, Georgia; BMBF, HGF and MPG, Germany; GSRI, Greece; RGC and Hong Kong SAR, China; ISF and Benoziyo Center, Israel; INFN, Italy; MEXT and JSPS, Japan; CNRST, Morocco; NWO, Netherlands; RCN, Norway; MEiN, Poland; FCT, Portugal; MNE/IFA, Romania; MESTD, Serbia; MSSR, Slovakia; ARRS and MIZŠ, Slovenia; DSI/NRF, South Africa; MICINN, Spain; SRC and Wallenberg Foundation, Sweden; SERI, SNSF and Cantons of Bern and Geneva, Switzerland; MOST, Taiwan; TENMAK, Türkiye; STFC, United Kingdom; DOE and NSF, United States of America. In addition, individual groups and members have received support from BCKDF, CANARIE, Compute Canada and CRC, Canada; PRIMUS 21/SCI/017 and UNCE SCI/013, Czech Republic; COST, ERC, ERDF, Horizon 2020 and Marie Skłodowska-Curie Actions, European Union; Investissements d'Avenir Labex, Investissements d'Avenir Idex and ANR, France; DFG and AvH Foundation, Germany; Herakleitos, Thales and Aristeia programmes co-financed by EU-ESF and the Greek NSRF, Greece; BSF-NSF and MINERVA, Israel; Norwegian Financial Mechanism 2014-2021, Norway; NCN and NAWA, Poland; La Caixa Banking Foundation, CERCA Programme Generalitat de Catalunya and PROMETEO and GenT Programmes Generalitat Valenciana, Spain; Göran Gustafssons Stiftelse, Sweden; The Royal Society and Leverhulme Trust, United Kingdom.

JHEP07(2023)125

The crucial computing support from all WLCG partners is acknowledged gratefully, in particular from CERN, the ATLAS Tier-1 facilities at TRIUMF (Canada), NDGF (Denmark, Norway, Sweden), CC-IN2P3 (France), KIT/GridKA (Germany), INFN-CNAF (Italy), NL-T1 (Netherlands), PIC (Spain), ASGC (Taiwan), RAL (U.K.) and BNL (U.S.A.), the Tier-2 facilities worldwide and large non-WLCG resource providers. Major contributors of computing resources are listed in ref. [76].

Open Access. This article is distributed under the terms of the Creative Commons Attribution License (CC-BY 4.0), which permits any use, distribution and reproduction in any medium, provided the original author(s) and source are credited.

References

[1] E. Eichten and K. Lane, *Low-scale technicolor at the Tevatron and LHC*, *Phys. Lett. B* **669** (2008) 235 [arXiv:0706.2339] [INSPIRE].

[2] N. Arkani-Hamed, A.G. Cohen, E. Katz and A.E. Nelson, *The littlest Higgs*, *JHEP* **07** (2002) 034 [hep-ph/0206021] [INSPIRE].

[3] D. Pappadopulo, A. Thamm, R. Torre and A. Wulzer, *Heavy vector triplets: bridging theory and data*, *JHEP* **09** (2014) 060 [arXiv:1402.4431] [INSPIRE].

[4] P. Artoisenet et al., *A framework for Higgs characterisation*, *JHEP* **11** (2013) 043 [arXiv:1306.6464] [INSPIRE].

[5] ATLAS collaboration, *Performance of top-quark and W-boson tagging with ATLAS in run 2 of the LHC*, *Eur. Phys. J. C* **79** (2019) 375 [arXiv:1808.07858] [INSPIRE].

[6] ATLAS collaboration, *Search for new resonances in $W\gamma$ and $Z\gamma$ final states in pp collisions at $\sqrt{s} = 8$ TeV with the ATLAS detector*, *Phys. Lett. B* **738** (2014) 428 [arXiv:1407.8150] [INSPIRE].

[7] ATLAS collaboration, *Search for heavy resonances decaying to a Z boson and a photon in pp collisions at $\sqrt{s} = 13$ TeV with the ATLAS detector*, *Phys. Lett. B* **764** (2017) 11 [arXiv:1607.06363] [INSPIRE].

[8] ATLAS collaboration, *Search for heavy resonances decaying to a photon and a hadronically decaying $Z/W/H$ boson in pp collisions at $\sqrt{s} = 13$ TeV with the ATLAS detector*, *Phys. Rev. D* **98** (2018) 032015 [arXiv:1805.01908] [INSPIRE].

[9] CMS collaboration, *Search for high-mass $Z\gamma$ resonances in $e^+e^-\gamma$ and $\mu^+\mu^-\gamma$ final states in proton-proton collisions at $\sqrt{s} = 8$ and 13 TeV*, *JHEP* **01** (2017) 076 [arXiv:1610.02960] [INSPIRE].

[10] CMS collaboration, *Search for high-mass $Z\gamma$ resonances in proton-proton collisions at $\sqrt{s} = 8$ and 13 TeV using jet substructure techniques*, *Phys. Lett. B* **772** (2017) 363 [arXiv:1612.09516] [INSPIRE].

[11] CMS collaboration, *Search for $Z\gamma$ resonances using leptonic and hadronic final states in proton-proton collisions at $\sqrt{s} = 13$ TeV*, *JHEP* **09** (2018) 148 [arXiv:1712.03143] [INSPIRE].

[12] CMS collaboration, *Search for $W\gamma$ resonances in proton-proton collisions at $\sqrt{s} = 13$ TeV using hadronic decays of Lorentz-boosted W bosons*, *Phys. Lett. B* **826** (2022) 136888 [arXiv:2106.10509] [INSPIRE].

JHEP07(2023)125

[13] ATLAS collaboration, *The ATLAS experiment at the CERN Large Hadron Collider*, 2008 *JINST* **3** S08003 [INSPIRE].

[14] ATLAS collaboration, *ATLAS Insertable B-Layer: technical design report*, ATLAS-TDR-19, CERN, Geneva, Switzerland (2010).

[15] ATLAS IBL collaboration, *Production and integration of the ATLAS Insertable B-Layer*, 2018 *JINST* **13** T05008 [arXiv:1803.00844] [INSPIRE].

[16] ATLAS collaboration, *Performance of the ATLAS trigger system in* 2015, *Eur. Phys. J. C* **77** (2017) 317 [arXiv:1611.09661] [INSPIRE].

[17] ATLAS collaboration, *The ATLAS collaboration software and firmware*, ATL-SOFT-PUB-2021-001, CERN, Geneva, Switzerland (2021).

[18] ATLAS collaboration, *Performance of electron and photon triggers in ATLAS during LHC run* 2, *Eur. Phys. J. C* **80** (2020) 47 [arXiv:1909.00761] [INSPIRE].

[19] ATLAS collaboration, *ATLAS data quality operations and performance for* 2015–2018 *data-taking*, 2020 *JINST* **15** P04003 [arXiv:1911.04632] [INSPIRE].

[20] ATLAS collaboration, *Luminosity determination in pp collisions at* $\sqrt{s} = 13$ *TeV using the ATLAS detector at the LHC*, ATLAS-CONF-2019-021, CERN, Geneva, Switzerland (2019).

[21] SHERPA collaboration, *Event generation with Sherpa* 2.2, *SciPost Phys.* **7** (2019) 034 [arXiv:1905.09127] [INSPIRE].

[22] T. Gleisberg and S. Höche, *Comix, a new matrix element generator*, *JHEP* **12** (2008) 039 [arXiv:0808.3674] [INSPIRE].

[23] F. Cascioli, P. Maierhofer and S. Pozzorini, *Scattering amplitudes with Open Loops*, *Phys. Rev. Lett.* **108** (2012) 111601 [arXiv:1111.5206] [INSPIRE].

[24] A. Denner, S. Dittmaier and L. Hofer, *Collier: a fortran-based Complex One-Loop LIbrary in Extended Regularizations*, *Comput. Phys. Commun.* **212** (2017) 220 [arXiv:1604.06792] [INSPIRE].

[25] S. Schumann and F. Krauss, *A parton shower algorithm based on Catani-Seymour dipole factorisation*, *JHEP* **03** (2008) 038 [arXiv:0709.1027] [INSPIRE].

[26] S. Catani, F. Krauss, R. Kuhn and B.R. Webber, *QCD matrix elements + parton showers*, *JHEP* **11** (2001) 063 [hep-ph/0109231] [INSPIRE].

[27] S. Höche, F. Krauss, S. Schumann and F. Siegert, *QCD matrix elements and truncated showers*, *JHEP* **05** (2009) 053 [arXiv:0903.1219] [INSPIRE].

[28] S. Höche, F. Krauss, M. Schönherr and F. Siegert, *A critical appraisal of NLO+PS matching methods*, *JHEP* **09** (2012) 049 [arXiv:1111.1220] [INSPIRE].

[29] S. Höche, F. Krauss, M. Schönherr and F. Siegert, *QCD matrix elements + parton showers: the NLO case*, *JHEP* **04** (2013) 027 [arXiv:1207.5030] [INSPIRE].

[30] NNPDF collaboration, *Parton distributions for the LHC run II*, *JHEP* **04** (2015) 040 [arXiv:1410.8849] [INSPIRE].

[31] H.-L. Lai et al., *New parton distributions for collider physics*, *Phys. Rev. D* **82** (2010) 074024 [arXiv:1007.2241] [INSPIRE].

JHEP07(2023)125

[32] J. Alwall et al., *The automated computation of tree-level and next-to-leading order differential cross sections, and their matching to parton shower simulations*, *JHEP* **07** (2014) 079 [arXiv:1405.0301] [INSPIRE].

[33] T. Sjöstrand, S. Mrenna and P.Z. Skands, *A brief introduction to PYTHIA* 8.1, *Comput. Phys. Commun.* **178** (2008) 852 [arXiv:0710.3820] [INSPIRE].

[34] R.D. Ball et al., *Parton distributions with LHC data*, *Nucl. Phys. B* **867** (2013) 244 [arXiv:1207.1303] [INSPIRE].

[35] ATLAS collaboration, *ATLAS Pythia* 8 *tunes to* 7 *TeV data*, ATL-PHYS-PUB-2014-021, CERN, Geneva, Switzerland (2014).

[36] E. Bagnaschi, G. Degrassi, P. Slavich and A. Vicini, *Higgs production via gluon fusion in the POWHEG approach in the SM and in the MSSM*, *JHEP* **02** (2012) 088 [arXiv:1111.2854] [INSPIRE].

[37] S. Alioli, P. Nason, C. Oleari and E. Re, *A general framework for implementing NLO calculations in shower Monte Carlo programs: the POWHEG BOX*, *JHEP* **06** (2010) 043 [arXiv:1002.2581] [INSPIRE].

[38] T. Sjöstrand et al., *An introduction to PYTHIA* 8.2, *Comput. Phys. Commun.* **191** (2015) 159 [arXiv:1410.3012] [INSPIRE].

[39] ATLAS collaboration, *Measurement of the Z/γ^* boson transverse momentum distribution in pp collisions at $\sqrt{s} = 7$ TeV with the ATLAS detector*, *JHEP* **09** (2014) 145 [arXiv:1406.3660] [INSPIRE].

[40] B.C. Allanach, J.P. Skittrall and K. Sridhar, *Z boson decay to photon plus Kaluza-Klein graviton in large extra dimensions*, *JHEP* **11** (2007) 089 [arXiv:0705.1953] [INSPIRE].

[41] A. Falkowski and J.F. Kamenik, *Diphoton portal to warped gravity*, *Phys. Rev. D* **94** (2016) 015008 [arXiv:1603.06980] [INSPIRE].

[42] B.M. Dillon and V. Sanz, *Kaluza-Klein gravitons at LHC*2, *Phys. Rev. D* **96** (2017) 035008 [arXiv:1603.09550] [INSPIRE].

[43] D.J. Lange, *The EvtGen particle decay simulation package*, *Nucl. Instrum. Meth. A* **462** (2001) 152 [INSPIRE].

[44] GEANT4 collaboration, *GEANT*4 — *a simulation toolkit*, *Nucl. Instrum. Meth. A* **506** (2003) 250 [INSPIRE].

[45] ATLAS collaboration, *The ATLAS simulation infrastructure*, *Eur. Phys. J. C* **70** (2010) 823 [arXiv:1005.4568] [INSPIRE].

[46] ATLAS collaboration, *The Pythia* 8 *A*3 *tune description of ATLAS minimum bias and inelastic measurements incorporating the Donnachie-Landshoff diffractive model*, ATL-PHYS-PUB-2016-017, CERN, Geneva, Switzerland (2016).

[47] ATLAS collaboration, *Electron and photon performance measurements with the ATLAS detector using the* 2015–2017 *LHC proton-proton collision data*, 2019 *JINST* **14** P12006 [arXiv:1908.00005] [INSPIRE].

[48] ATLAS collaboration, *Optimisation of large-radius jet reconstruction for the ATLAS detector in* 13 *TeV proton-proton collisions*, *Eur. Phys. J. C* **81** (2021) 334 [arXiv:2009.04986] [INSPIRE].

JHEP07(2023)125

[49] M. Cacciari, G.P. Salam and G. Soyez, *The anti-k_t jet clustering algorithm*, *JHEP* **04** (2008) 063 [arXiv:0802.1189] [INSPIRE].

[50] M. Cacciari, G.P. Salam and G. Soyez, *FastJet user manual*, *Eur. Phys. J. C* **72** (2012) 1896 [arXiv:1111.6097] [INSPIRE].

[51] D. Krohn, J. Thaler and L.-T. Wang, *Jet trimming*, *JHEP* **02** (2010) 084 [arXiv:0912.1342] [INSPIRE].

[52] S.D. Ellis and D.E. Soper, *Successive combination jet algorithm for hadron collisions*, *Phys. Rev. D* **48** (1993) 3160 [hep-ph/9305266] [INSPIRE].

[53] ATLAS collaboration, *In situ calibration of large-radius jet energy and mass in 13 TeV proton-proton collisions with the ATLAS detector*, *Eur. Phys. J. C* **79** (2019) 135 [arXiv:1807.09477] [INSPIRE].

[54] ATLAS collaboration, *Improving jet substructure performance in ATLAS using Track-CaloClusters*, ATL-PHYS-PUB-2017-015, CERN, Geneva, Switzerland (2017).

[55] ATLAS collaboration, *Search for heavy diboson resonances in semileptonic final states in pp collisions at $\sqrt{s} = 13$ TeV with the ATLAS detector*, *Eur. Phys. J. C* **80** (2020) 1165 [arXiv:2004.14636] [INSPIRE].

[56] A.J. Larkoski, G.P. Salam and J. Thaler, *Energy correlation functions for jet substructure*, *JHEP* **06** (2013) 108 [arXiv:1305.0007] [INSPIRE].

[57] A.J. Larkoski, I. Moult and D. Neill, *Power counting to better jet observables*, *JHEP* **12** (2014) 009 [arXiv:1409.6298] [INSPIRE].

[58] ATLAS collaboration, *Measurements of b-jet tagging efficiency with the ATLAS detector using $t\bar{t}$ events at $\sqrt{s} = 13$ TeV*, *JHEP* **08** (2018) 089 [arXiv:1805.01845] [INSPIRE].

[59] M. Cacciari and G.P. Salam, *Pileup subtraction using jet areas*, *Phys. Lett. B* **659** (2008) 119 [arXiv:0707.1378] [INSPIRE].

[60] ATLAS collaboration, *Variable radius, exclusive-k_T, and center-of-mass subjet reconstruction for Higgs($\to b\bar{b}$) tagging in ATLAS*, ATL-PHYS-PUB-2017-010, CERN, Geneva, Switzerland (2017).

[61] ATLAS collaboration, *ATLAS b-jet identification performance and efficiency measurement with $t\bar{t}$ events in pp collisions at $\sqrt{s} = 13$ TeV*, *Eur. Phys. J. C* **79** (2019) 970 [arXiv:1907.05120] [INSPIRE].

[62] CDF collaboration, *Search for new particles decaying into dijets in proton-antiproton collisions at $\sqrt{s} = 1.96$ TeV*, *Phys. Rev. D* **79** (2009) 112002 [arXiv:0812.4036] [INSPIRE].

[63] ATLAS collaboration, *Measurement of Higgs boson production in the diphoton decay channel in pp collisions at center-of-mass energies of 7 and 8 TeV with the ATLAS detector*, *Phys. Rev. D* **90** (2014) 112015 [arXiv:1408.7084] [INSPIRE].

[64] ATLAS collaboration, *Search for resonances in diphoton events at $\sqrt{s} = 13$ TeV with the ATLAS detector*, *JHEP* **09** (2016) 001 [arXiv:1606.03833] [INSPIRE].

[65] G. Avoni et al., *The new LUCID-2 detector for luminosity measurement and monitoring in ATLAS*, 2018 *JINST* **13** P07017 [INSPIRE].

[66] ATLAS collaboration, *Luminosity determination in pp collisions at $\sqrt{s} = 8$ TeV using the ATLAS detector at the LHC*, *Eur. Phys. J. C* **76** (2016) 653 [arXiv:1608.03953] [INSPIRE].

JHEP07(2023)125

[67] ATLAS collaboration, *Simulation-based extrapolation of b-tagging calibrations towards high transverse momenta in the ATLAS experiment*, ATL-PHYS-PUB-2021-003, CERN, Geneva, Switzerland (2021).

[68] A. Buckley et al., *LHAPDF6: parton density access in the LHC precision era*, *Eur. Phys. J. C* **75** (2015) 132 [arXiv:1412.7420] [INSPIRE].

[69] W. Verkerke and D.P. Kirkby, *The RooFit toolkit for data modeling*, *eConf* **C0303241** (2003) MOLT007 [physics/0306116] [INSPIRE].

[70] L. Moneta et al., *The RooStats project*, *PoS* **ACAT2010** (2010) 057 [arXiv:1009.1003] [INSPIRE].

[71] G. Cowan, K. Cranmer, E. Gross and O. Vitells, *Asymptotic formulae for likelihood-based tests of new physics*, *Eur. Phys. J. C* **71** (2011) 1554 [*Erratum ibid.* **73** (2013) 2501] [arXiv:1007.1727] [INSPIRE].

[72] T. Junk, *Confidence level computation for combining searches with small statistics*, *Nucl. Instrum. Meth. A* **434** (1999) 435 [hep-ex/9902006] [INSPIRE].

[73] A.L. Read, *Presentation of search results: the CL_s technique*, *J. Phys. G* **28** (2002) 2693 [INSPIRE].

[74] Particle Data Group collaboration, *Review of particle physics*, *PTEP* **2020** (2020) 083C01 [INSPIRE].

[75] G. Choudalakis and D. Casadei, *Plotting the differences between data and expectation*, *Eur. Phys. J. Plus* **127** (2012) 25 [arXiv:1111.2062] [INSPIRE].

[76] ATLAS collaboration, *ATLAS computing acknowledgements*, ATL-SOFT-PUB-2021-003, CERN, Geneva, Switzerland (2021).

JHEP07(2023)125

The ATLAS collaboration

G. Aad[99], B. Abbott[117], D.C. Abbott[100], A. Abed Abud[34], K. Abeling[53], D.K. Abhayasinghe[92], S.H. Abidi[27], A. Aboulhorma[33e], H. Abramowicz[148], H. Abreu[147], Y. Abulaiti[5], A.C. Abusleme Hoffman[134a], B.S. Acharya[66a,66b,p], B. Achkar[53], L. Adam[97], C. Adam Bourdarios[4], L. Adamczyk[82a], L. Adamek[152], S.V. Addepalli[24], J. Adelman[112], A. Adiguzel[11c,ab], S. Adorni[54], T. Adye[131], A.A. Affolder[133], Y. Afik[34], C. Agapopoulou[64], M.N. Agaras[12], J. Agarwala[70a,70b], A. Aggarwal[110], C. Agheorghiesei[25c], J.A. Aguilar-Saavedra[127f,127a,aa], A. Ahmad[34], F. Ahmadov[36,y], W.S. Ahmed[101], X. Ai[46], G. Aielli[73a,73b], I. Aizenberg[165], S. Akatsuka[84], M. Akbiyik[97], T.P.A. Åkesson[95], A.V. Akimov[35], K. Al Khoury[39], G.L. Alberghi[21b], J. Albert[161], P. Albicocco[51], M.J. Alconada Verzini[87], S. Alderweireldt[50], M. Aleksa[34], I.N. Aleksandrov[36], C. Alexa[25b], T. Alexopoulos[9], A. Alfonsi[111], F. Alfonsi[21b], M. Alhroob[117], B. Ali[129], S. Ali[145], M. Aliev[35], G. Alimonti[68a], C. Allaire[34], B.M.M. Allbrooke[143], P.P. Allport[19], A. Aloisio[69a,69b], F. Alonso[87], C. Alpigiani[135], E. Alunno Camelia[73a,73b], M. Alvarez Estevez[96], M.G. Alviggi[69a,69b], Y. Amaral Coutinho[79b], A. Ambler[101], L. Ambroz[123], C. Amelung[34], D. Amidei[103], S.P. Amor Dos Santos[127a], S. Amoroso[46], K.R. Amos[159], C.S. Amrouche[54], V. Ananiev[122], C. Anastopoulos[136], N. Andari[132], T. Andeen[10], J.K. Anders[18], S.Y. Andrean[45a,45b], A. Andreazza[68a,68b], S. Angelidakis[8], A. Angerami[39], A.V. Anisenkov[35], A. Annovi[71a], C. Antel[54], M.T. Anthony[136], E. Antipov[118], M. Antonelli[51], D.J.A. Antrim[16a], F. Anulli[72a], M. Aoki[80], J.A. Aparisi Pozo[159], M.A. Aparo[143], L. Aperio Bella[46], N. Aranzabal[34], V. Araujo Ferraz[79a], C. Arcangeletti[51], A.T.H. Arce[49], E. Arena[89], J-F. Arguin[105], S. Argyropoulos[52], J.-H. Arling[46], A.J. Armbruster[34], A. Armstrong[156], O. Arnaez[152], H. Arnold[34], Z.P. Arrubarrena Tame[106], G. Artoni[123], H. Asada[108], K. Asai[115], S. Asai[150], N.A. Asbah[59], E.M. Asimakopoulou[157], L. Asquith[143], J. Assahsah[33d], K. Assamagan[27], R. Astalos[26a], R.J. Atkin[31a], M. Atkinson[158], N.B. Atlay[17], H. Atmani[60b], P.A. Atmasiddha[103], K. Augsten[129], S. Auricchio[69a,69b], V.A. Austrup[167], G. Avner[147], G. Avolio[34], M.K. Ayoub[13c], G. Azuelos[105,ai], D. Babal[26a], H. Bachacou[132], K. Bachas[149], A. Bachiu[32], F. Backman[45a,45b], A. Badea[59], P. Bagnaia[72a,72b], H. Bahrasemani[139], A.J. Bailey[159], V.R. Bailey[158], J.T. Baines[131], C. Bakalis[9], O.K. Baker[168], P.J. Bakker[111], E. Bakos[14], D. Bakshi Gupta[7], S. Balaji[144], R. Balasubramanian[111], E.M. Baldin[35], P. Balek[130], E. Ballabene[68a,68b], F. Balli[132], L.M. Baltes[61a], W.K. Balunas[123], J. Balz[97], E. Banas[83], M. Bandieramonte[126], A. Bandyopadhyay[22], S. Bansal[22], L. Barak[148], E.L. Barberio[102], D. Barberis[55b,55a], M. Barbero[99], G. Barbour[93], K.N. Barends[31a], T. Barillari[107], M-S. Barisits[34], J. Barkeloo[120], T. Barklow[140], B.M. Barnett[131], R.M. Barnett[16a], A. Baroncelli[60a], G. Barone[27], A.J. Barr[123], L. Barranco Navarro[45a,45b], F. Barreiro[96], J. Barreiro Guimarães da Costa[13a], U. Barron[148], S. Barsov[35], F. Bartels[61a], R. Bartoldus[140], G. Bartolini[99], A.E. Barton[88], P. Bartos[26a], A. Basalaev[46], A. Basan[97], M. Baselga[46], I. Bashta[74a,74b], A. Bassalat[64,ae], M.J. Basso[152], C.R. Basson[98], R.L. Bates[57], S. Batlamous[33e], J.R. Batley[30], B. Batool[138],

JHEP07(2023)125

M. Battaglia[133], M. Bauce[72a,72b], F. Bauer[132,*], P. Bauer[22], H.S. Bawa[29], A. Bayirli[11c], J.B. Beacham[49], T. Beau[124], P.H. Beauchemin[155], F. Becherer[52], P. Bechtle[22], H.P. Beck[18,r], K. Becker[163], C. Becot[46], A.J. Beddall[11a], V.A. Bednyakov[36], C.P. Bee[142], T.A. Beermann[34], M. Begalli[79b], M. Begel[27], A. Behera[142], J.K. Behr[46], C. Beirao Da Cruz E Silva[34], J.F. Beirer[53,34], F. Beisiegel[22], M. Belfkir[4], G. Bella[148], L. Bellagamba[21b], A. Bellerive[32], P. Bellos[19], K. Beloborodov[35], K. Belotskiy[35], N.L. Belyaev[35], D. Benchekroun[33a], Y. Benhammou[148], D.P. Benjamin[27], M. Benoit[27], J.R. Bensinger[24], S. Bentvelsen[111], L. Beresford[34], M. Beretta[51], D. Berge[17], E. Bergeaas Kuutmann[157], N. Berger[4], B. Bergmann[129], L.J. Bergsten[24], J. Beringer[16a], S. Berlendis[6], G. Bernardi[124], C. Bernius[140], F.U. Bernlochner[22], T. Berry[92], P. Berta[130], A. Berthold[48], I.A. Bertram[88], O. Bessidskaia Bylund[167], S. Bethke[107], A. Betti[42], A.J. Bevan[91], S. Bhatta[142], D.S. Bhattacharya[162], P. Bhattarai[24], V.S. Bhopatkar[5], R. Bi[126], R.M. Bianchi[126], O. Biebel[106], R. Bielski[120], N.V. Biesuz[71a,71b], M. Biglietti[74a], T.R.V. Billoud[129], M. Bindi[53], A. Bingul[11d], C. Bini[72a,72b], S. Biondi[21b,21a], A. Biondini[89], C.J. Birch-sykes[98], G.A. Bird[19,131], M. Birman[165], T. Bisanz[34], D. Biswas[166,k], A. Bitadze[98], C. Bittrich[48], K. Bjørke[122], I. Bloch[46], C. Blocker[24], A. Blue[57], U. Blumenschein[91], J. Blumenthal[97], G.J. Bobbink[111], V.S. Bobrovnikov[35], M. Boehler[52], D. Bogavac[12], A.G. Bogdanchikov[35], C. Bohm[45a], V. Boisvert[92], P. Bokan[46], T. Bold[82a], M. Bomben[124], M. Bona[91], M. Boonekamp[132], C.D. Booth[92], A.G. Borbély[57], H.M. Borecka-Bielska[105], L.S. Borgna[93], G. Borissov[88], D. Bortoletto[123], D. Boscherini[21b], M. Bosman[12], J.D. Bossio Sola[34], K. Bouaouda[33a], J. Boudreau[126], E.V. Bouhova-Thacker[88], D. Boumediene[38], R. Bouquet[124], A. Boveia[116], J. Boyd[34], D. Boye[27], I.R. Boyko[36], A.J. Bozson[92], J. Bracinik[19], N. Brahimi[60d,60c], G. Brandt[167], O. Brandt[30], F. Braren[46], B. Brau[100], J.E. Brau[120], W.D. Breaden Madden[57], K. Brendlinger[46], R. Brener[165], L. Brenner[34], R. Brenner[157], S. Bressler[165], B. Brickwedde[97], D.L. Briglin[19], D. Britton[57], D. Britzger[107], I. Brock[22], R. Brock[104], G. Brooijmans[39], W.K. Brooks[134f], E. Brost[27], P.A. Bruckman de Renstrom[83], B. Brüers[46], D. Bruncko[26b,*], A. Bruni[21b], G. Bruni[21b], M. Bruschi[21b], N. Bruscino[72a,72b], L. Bryngemark[140], T. Buanes[15], Q. Buat[142], P. Buchholz[138], A.G. Buckley[57], I.A. Budagov[36,*], M.K. Bugge[122], O. Bulekov[35], B.A. Bullard[59], S. Burdin[89], C.D. Burgard[46], A.M. Burger[118], B. Burghgrave[7], J.T.P. Burr[46], C.D. Burton[10], J.C. Burzynski[139], E.L. Busch[39], V. Büscher[97], P.J. Bussey[57], J.M. Butler[23], C.M. Buttar[57], J.M. Butterworth[93], W. Buttinger[131], C.J. Buxo Vazquez[104], A.R. Buzykaev[35], G. Cabras[21b], S. Cabrera Urbán[159], D. Caforio[56], H. Cai[126], V.M.M. Cairo[140], O. Cakir[3a], N. Calace[34], P. Calafiura[16a], G. Calderini[124], P. Calfayan[65], G. Callea[57], L.P. Caloba[79b], D. Calvet[38], S. Calvet[38], T.P. Calvet[99], M. Calvetti[71a,71b], R. Camacho Toro[124], S. Camarda[34], D. Camarero Munoz[96], P. Camarri[73a,73b], M.T. Camerlingo[74a,74b], D. Cameron[122], C. Camincher[161], M. Campanelli[93], A. Camplani[40], V. Canale[69a,69b], A. Canesse[101], M. Cano Bret[77], J. Cantero[118], Y. Cao[158], F. Capocasa[24], M. Capua[41b,41a], A. Carbone[68a,68b], R. Cardarelli[73a], J.C.J. Cardenas[7], F. Cardillo[159], T. Carli[34], G. Carlino[69a], B.T. Carlson[126], E.M. Carlson[161,153a], L. Carminati[68a,68b],

JHEP07(2023)125

M. Carnesale[72a,72b], R.M.D. Carney[140], S. Caron[110], E. Carquin[134f], S. Carrá[46], G. Carratta[21b,21a], J.W.S. Carter[152], T.M. Carter[50], D. Casadei[31c], M.P. Casado[12,h], A.F. Casha[152], E.G. Castiglia[168], F.L. Castillo[61a], L. Castillo Garcia[12], V. Castillo Gimenez[159], N.F. Castro[127a,127e], A. Catinaccio[34], J.R. Catmore[122], A. Cattai[34], V. Cavaliere[27], N. Cavalli[21b,21a], V. Cavasinni[71a,71b], E. Celebi[11b], F. Celli[123], M.S. Centonze[67a,67b], K. Cerny[119], A.S. Cerqueira[79a], A. Cerri[143], L. Cerrito[73a,73b], F. Cerutti[16a], A. Cervelli[21b], S.A. Cetin[11b], Z. Chadi[33a], D. Chakraborty[112], M. Chala[127f], J. Chan[166], W.S. Chan[111], W.Y. Chan[89], J.D. Chapman[30], B. Chargeishvili[146b], D.G. Charlton[19], T.P. Charman[91], M. Chatterjee[18], S. Chekanov[5], S.V. Chekulaev[153a], G.A. Chelkov[36,a], A. Chen[103], B. Chen[148], B. Chen[161], C. Chen[60a], C.H. Chen[78], H. Chen[13c], H. Chen[27], J. Chen[60c], J. Chen[24], S. Chen[125], S.J. Chen[13c], X. Chen[60c], X. Chen[13b,ah], Y. Chen[60a], Y-H. Chen[46], C.L. Cheng[166], H.C. Cheng[62a], A. Cheplakov[36], E. Cheremushkina[46], E. Cherepanova[36], R. Cherkaoui El Moursli[33e], E. Cheu[6], K. Cheung[63], L. Chevalier[132], V. Chiarella[51], G. Chiarelli[71a], G. Chiodini[67a], A.S. Chisholm[19], A. Chitan[25b], Y.H. Chiu[161], M.V. Chizhov[36,s], K. Choi[10], A.R. Chomont[72a,72b], Y. Chou[100], E.Y.S. Chow[111], T. Chowdhury[31f], L.D. Christopher[31f], M.C. Chu[62a], X. Chu[13a,13d], J. Chudoba[128], J.J. Chwastowski[83], D. Cieri[107], K.M. Ciesla[83], V. Cindro[90], I.A. Cioară[25b], A. Ciocio[16a], F. Cirotto[69a,69b], Z.H. Citron[165,l], M. Citterio[68a], D.A. Ciubotaru[25b], B.M. Ciungu[152], A. Clark[54], P.J. Clark[50], J.M. Clavijo Columbie[46], S.E. Clawson[98], C. Clement[45a,45b], L. Clissa[21b,21a], Y. Coadou[99], M. Cobal[66a,66c], A. Coccaro[55b], J. Cochran[78], R.F. Coelho Barrue[127a], R. Coelho Lopes De Sa[100], S. Coelli[68a], H. Cohen[148], A.E.C. Coimbra[34], B. Cole[39], J. Collot[58], P. Conde Muiño[127a,127g], S.H. Connell[31c], I.A. Connelly[57], E.I. Conroy[123], F. Conventi[69a,aj], H.G. Cooke[19], A.M. Cooper-Sarkar[123], F. Cormier[160], L.D. Corpe[34], M. Corradi[72a,72b], E.E. Corrigan[95], F. Corriveau[101,x], M.J. Costa[159], F. Costanza[4], D. Costanzo[136], B.M. Cote[116], G. Cowan[92], J.W. Cowley[30], K. Cranmer[114], S. Crépé-Renaudin[58], F. Crescioli[124], M. Cristinziani[138], M. Cristoforetti[75a,75b,c], V. Croft[155], G. Crosetti[41b,41a], A. Cueto[34], T. Cuhadar Donszelmann[156], H. Cui[13a,13d], A.R. Cukierman[140], W.R. Cunningham[57], F. Curcio[41b,41a], P. Czodrowski[34], M.M. Czurylo[61b], M.J. Da Cunha Sargedas De Sousa[60a], J.V. Da Fonseca Pinto[79b], C. Da Via[98], W. Dabrowski[82a], T. Dado[47], S. Dahbi[31f], T. Dai[103], C. Dallapiccola[100], M. Dam[40], G. D'amen[27], V. D'Amico[74a,74b], J. Damp[97], J.R. Dandoy[125], M.F. Daneri[28], M. Danninger[139], V. Dao[34], G. Darbo[55b], S. Darmora[5], A. Dattagupta[120], S. D'Auria[68a,68b], C. David[153b], T. Davidek[130], D.R. Davis[49], B. Davis-Purcell[32], I. Dawson[91], K. De[7], R. De Asmundis[69a], M. De Beurs[111], S. De Castro[21b,21a], N. De Groot[110], P. de Jong[111], H. De la Torre[104], A. De Maria[13c], D. De Pedis[72a], A. De Salvo[72a], U. De Sanctis[73a,73b], M. De Santis[73a,73b], A. De Santo[143], J.B. De Vivie De Regie[58], D.V. Dedovich[36], J. Degens[111], A.M. Deiana[42], J. Del Peso[96], Y. Delabat Diaz[46], F. Deliot[132], C.M. Delitzsch[6], M. Della Pietra[69a,69b], D. Della Volpe[54], A. Dell'Acqua[34], L. Dell'Asta[68a,68b], M. Delmastro[4], P.A. Delsart[58], S. Demers[168], M. Demichev[36],

JHEP07(2023)125

S.P. Denisov[35], L. D'Eramo[112], D. Derendarz[83], J.E. Derkaoui[33d], F. Derue[124], P. Dervan[89], K. Desch[22], K. Dette[152], C. Deutsch[22], P.O. Deviveiros[34], F.A. Di Bello[72a,72b], A. Di Ciaccio[73a,73b], L. Di Ciaccio[4], A. Di Domenico[72a,72b], C. Di Donato[69a,69b], A. Di Girolamo[34], G. Di Gregorio[71a,71b], A. Di Luca[75a,75b], B. Di Micco[74a,74b], R. Di Nardo[74a,74b], C. Diaconu[99], F.A. Dias[111], T. Dias Do Vale[127a], M.A. Diaz[134a,134b], F.G. Diaz Capriles[22], J. Dickinson[16a], M. Didenko[159], E.B. Diehl[103], J. Dietrich[17], S. Díez Cornell[46], C. Diez Pardos[138], A. Dimitrievska[16a], W. Ding[13b], J. Dingfelder[22], I-M. Dinu[25b], S.J. Dittmeier[61b], F. Dittus[34], F. Djama[99], T. Djobava[146b], J.I. Djuvsland[15], M.A.B. Do Vale[79c], D. Dodsworth[24], C. Doglioni[95], J. Dolejsi[130], Z. Dolezal[130], M. Donadelli[79d], B. Dong[60c], J. Donini[38], A. D'Onofrio[13c], M. D'Onofrio[89], J. Dopke[131], A. Doria[69a], M.T. Dova[87], A.T. Doyle[57], E. Drechsler[139], E. Dreyer[139], T. Dreyer[53], A.S. Drobac[155], D. Du[60a], T.A. du Pree[111], F. Dubinin[35], M. Dubovsky[26a], A. Dubreuil[54], E. Duchovni[165], G. Duckeck[106], O.A. Ducu[34,25b], D. Duda[107], A. Dudarev[34], M. D'uffizi[98], L. Duflot[64], M. Dührssen[34], C. Dülsen[167], A.E. Dumitriu[25b], M. Dunford[61a], S. Dungs[47], K. Dunne[45a,45b], A. Duperrin[99], H. Duran Yildiz[3a], M. Düren[56], A. Durglishvili[146b], B. Dutta[46], B.L. Dwyer[112], G.I. Dyckes[16a], M. Dyndal[82a], S. Dysch[98], B.S. Dziedzic[83], B. Eckerova[26a], M.G. Eggleston[49], E. Egidio Purcino De Souza[79b], L.F. Ehrke[54], T. Eifert[7], G. Eigen[15], K. Einsweiler[16a], T. Ekelof[157], Y. El Ghazali[33b], H. El Jarrari[33e], A. El Moussaouy[33a], V. Ellajosyula[157], M. Ellert[157], F. Ellinghaus[167], A.A. Elliot[91], N. Ellis[34], J. Elmsheuser[27], M. Elsing[34], D. Emeliyanov[131], A. Emerman[39], Y. Enari[150], J. Erdmann[47], A. Ereditato[18], P.A. Erland[83], M. Errenst[167], M. Escalier[64], C. Escobar[159], O. Estrada Pastor[159], E. Etzion[148], G. Evans[127a], H. Evans[65], M.O. Evans[143], A. Ezhilov[35], F. Fabbri[57], L. Fabbri[21b,21a], G. Facini[163], V. Fadeyev[133], R.M. Fakhrutdinov[35], S. Falciano[72a], P.J. Falke[22], S. Falke[34], J. Faltova[130], Y. Fan[13a], Y. Fang[13a,13d], G. Fanourakis[44], M. Fanti[68a,68b], M. Faraj[60c], A. Farbin[7], A. Farilla[74a], E.M. Farina[70a,70b], T. Farooque[104], S.M. Farrington[50], P. Farthouat[34], F. Fassi[33e], D. Fassouliotis[8], M. Faucci Giannelli[73a,73b], W.J. Fawcett[30], L. Fayard[64], O.L. Fedin[35,a], M. Feickert[158], L. Feligioni[99], A. Fell[136], C. Feng[60b], M. Feng[13b], M.J. Fenton[156], A.B. Fenyuk[35], S.W. Ferguson[43], J. Ferrando[46], A. Ferrari[157], P. Ferrari[111], R. Ferrari[70a], D. Ferrere[54], C. Ferretti[103], F. Fiedler[97], A. Filipčič[90], F. Filthaut[110], M.C.N. Fiolhais[127a,127c,b], L. Fiorini[159], F. Fischer[138], W.C. Fisher[104], T. Fitschen[19], I. Fleck[138], P. Fleischmann[103], T. Flick[167], B.M. Flierl[106], L. Flores[125], M. Flores[31d,ad], L.R. Flores Castillo[62a], F.M. Follega[75a,75b], N. Fomin[15], J.H. Foo[152], B.C. Forland[65], A. Formica[132], F.A. Förster[12], A.C. Forti[98], E. Fortin[99], M.G. Foti[123], L. Fountas[8,i], D. Fournier[64], H. Fox[88], P. Francavilla[71a,71b], S. Francescato[59], M. Franchini[21b,21a], S. Franchino[61a], D. Francis[34], L. Franco[4], L. Franconi[18], M. Franklin[59], G. Frattari[72a,72b], A.C. Freegard[91], P.M. Freeman[19], W.S. Freund[79b], E.M. Freundlich[47], D. Froidevaux[34], J.A. Frost[123], Y. Fu[60a], M. Fujimoto[115], E. Fullana Torregrosa[159,*], J. Fuster[159], A. Gabrielli[21b,21a], A. Gabrielli[34], P. Gadow[46], G. Gagliardi[55b,55a], L.G. Gagnon[16a], G.E. Gallardo[123], E.J. Gallas[123], B.J. Gallop[131], R. Gamboa Goni[91], K.K. Gan[116], S. Ganguly[150], J. Gao[60a], Y. Gao[50], Y.S. Gao[29,n],

JHEP07(2023)125

F.M. Garay Walls[134a], C. García[159], J.E. García Navarro[159], J.A. García Pascual[13a], M. Garcia-Sciveres[16a], R.W. Gardner[37], D. Garg[77], R.B. Garg[140,q], S. Gargiulo[52], C.A. Garner[152], V. Garonne[122], S.J. Gasiorowski[135], P. Gaspar[79b], G. Gaudio[70a], P. Gauzzi[72a,72b], I.L. Gavrilenko[35], A. Gavrilyuk[35], C. Gay[160], G. Gaycken[46], E.N. Gazis[9], A.A. Geanta[25b], C.M. Gee[133], C.N.P. Gee[131], J. Geisen[95], M. Geisen[97], C. Gemme[55b], M.H. Genest[58], S. Gentile[72a,72b], S. George[92], W.F. George[19], T. Geralis[44], L.O. Gerlach[53], P. Gessinger-Befurt[34], M. Ghasemi Bostanabad[161], M. Ghneimat[138], A. Ghosh[156], A. Ghosh[77], B. Giacobbe[21b], S. Giagu[72a,72b], N. Giangiacomi[152], P. Giannetti[71a], A. Giannini[69a,69b], S.M. Gibson[92], M. Gignac[133], D.T. Gil[82b], B.J. Gilbert[39], D. Gillberg[32], G. Gilles[111], N.E.K. Gillwald[46], D.M. Gingrich[2,ai], M.P. Giordani[66a,66c], P.F. Giraud[132], G. Giugliarelli[66a,66c], D. Giugni[68a], F. Giuli[73a,73b], I. Gkialas[8,i], P. Gkountoumis[9], L.K. Gladilin[35], C. Glasman[96], G.R. Gledhill[120], M. Glisic[120], I. Gnesi[41b,e], M. Goblirsch-Kolb[24], D. Godin[105], S. Goldfarb[102], T. Golling[54], D. Golubkov[35], J.P. Gombas[104], A. Gomes[127a,127b], R. Goncalves Gama[53], R. Gonçalo[127a,127c], G. Gonella[120], L. Gonella[19], A. Gongadze[36], F. Gonnella[19], J.L. Gonski[39], R.Y. González Andana[134a], S. González de la Hoz[159], S. Gonzalez Fernandez[12], R. Gonzalez Lopez[89], C. Gonzalez Renteria[16a], R. Gonzalez Suarez[157], S. Gonzalez-Sevilla[54], G.R. Gonzalvo Rodriguez[159], L. Goossens[34], N.A. Gorasia[19], P.A. Gorbounov[35], B. Gorini[34], E. Gorini[67a,67b], A. Gorišek[90], A.T. Goshaw[49], M.I. Gostkin[36], C.A. Gottardo[110], M. Gouighri[33b], V. Goumarre[46], A.G. Goussiou[135], N. Govender[31c], C. Goy[4], I. Grabowska-Bold[82a], K. Graham[32], E. Gramstad[122], S. Grancagnolo[17], M. Grandi[143], V. Gratchev[35,*], P.M. Gravila[25f], F.G. Gravili[67a,67b], H.M. Gray[16a], C. Grefe[22], I.M. Gregor[46], P. Grenier[140], K. Grevtsov[46], C. Grieco[12], N.A. Grieser[117], A.A. Grillo[133], K. Grimm[29,m], S. Grinstein[12,u], J.-F. Grivaz[64], S. Groh[97], E. Gross[165], J. Grosse-Knetter[53], C. Grud[103], A. Grummer[109], J.C. Grundy[123], L. Guan[103], W. Guan[166], C. Gubbels[160], J. Guenther[34], J.G.R. Guerrero Rojas[159], F. Guescini[107], R. Gugel[97], A. Guida[46], T. Guillemin[4], S. Guindon[34], J. Guo[60c], L. Guo[64], Y. Guo[103], R. Gupta[46], S. Gurbuz[22], G. Gustavino[117], M. Guth[54], P. Gutierrez[117], L.F. Gutierrez Zagazeta[125], C. Gutschow[93], C. Guyot[132], C. Gwenlan[123], C.B. Gwilliam[89], E.S. Haaland[122], A. Haas[114], M. Habedank[46], C. Haber[16a], H.K. Hadavand[7], A. Hadef[97], S. Hadzic[107], M. Haleem[162], J. Haley[118], J.J. Hall[136], G. Halladjian[104], G.D. Hallewell[99], L. Halser[18], K. Hamano[161], H. Hamdaoui[33e], M. Hamer[22], G.N. Hamity[50], K. Han[60a], L. Han[13c], L. Han[60a], S. Han[16a], Y.F. Han[152], K. Hanagaki[80], M. Hance[133], M.D. Hank[37], R. Hankache[98], E. Hansen[95], J.B. Hansen[40], J.D. Hansen[40], M.C. Hansen[22], P.H. Hansen[40], K. Hara[154], T. Harenberg[167], S. Harkusha[35], Y.T. Harris[123], P.F. Harrison[163], N.M. Hartman[140], N.M. Hartmann[106], Y. Hasegawa[137], A. Hasib[50], S. Hassani[132], S. Haug[18], R. Hauser[104], M. Havranek[129], C.M. Hawkes[19], R.J. Hawkings[34], S. Hayashida[108], D. Hayden[104], C. Hayes[103], R.L. Hayes[160], C.P. Hays[123], J.M. Hays[91], H.S. Hayward[89], S.J. Haywood[131], F. He[60a], Y. He[151], Y. He[124], M.P. Heath[50], V. Hedberg[95], A.L. Heggelund[122], N.D. Hehir[91], C. Heidegger[52], K.K. Heidegger[52], W.D. Heidorn[78], J. Heilman[32], S. Heim[46], T. Heim[16a],

JHEP07(2023)125

B. Heinemann[46,af], J.G. Heinlein[125], J.J. Heinrich[120], L. Heinrich[34], J. Hejbal[128], L. Helary[46], A. Held[114], S. Hellesund[122], C.M. Helling[133], S. Hellman[45a,45b], C. Helsens[34], R.C.W. Henderson[88], L. Henkelmann[30], A.M. Henriques Correia[34], H. Herde[140], Y. Hernández Jiménez[142], H. Herr[97], M.G. Herrmann[106], T. Herrmann[48], G. Herten[52], R. Hertenberger[106], L. Hervas[34], N.P. Hessey[153a], H. Hibi[81], S. Higashino[80], E. Higón-Rodriguez[159], K.H. Hiller[46], S.J. Hillier[19], M. Hils[48], I. Hinchliffe[16a], F. Hinterkeuser[22], M. Hirose[121], S. Hirose[154], D. Hirschbuehl[167], B. Hiti[90], O. Hladik[128], J. Hobbs[142], R. Hobincu[25e], N. Hod[165], M.C. Hodgkinson[136], B.H. Hodkinson[30], A. Hoecker[34], J. Hofer[46], D. Hohn[52], T. Holm[22], T.R. Holmes[37], M. Holzbock[107], L.B.A.H. Hommels[30], B.P. Honan[98], J. Hong[60c], T.M. Hong[126], Y. Hong[53], J.C. Honig[52], A. Hönle[107], B.H. Hooberman[158], W.H. Hopkins[5], Y. Horii[108], L.A. Horyn[37], S. Hou[145], J. Howarth[57], J. Hoya[87], M. Hrabovsky[119], A. Hrynevich[35], T. Hryn'ova[4], P.J. Hsu[63], S.-C. Hsu[135], Q. Hu[39], S. Hu[60c], Y.F. Hu[13a,13d,ak], D.P. Huang[93], X. Huang[13c], Y. Huang[60a], Y. Huang[13a], Z. Hubacek[129], F. Hubaut[99], M. Huebner[22], F. Huegging[22], T.B. Huffman[123], M. Huhtinen[34], S.K. Huiberts[15], R. Hulsken[58], N. Huseynov[36,y], J. Huston[104], J. Huth[59], R. Hyneman[140], S. Hyrych[26a], G. Iacobucci[54], G. Iakovidis[27], I. Ibragimov[138], L. Iconomidou-Fayard[64], P. Iengo[34], R. Iguchi[150], T. Iizawa[54], Y. Ikegami[80], A. Ilg[18], N. Ilic[152], H. Imam[33a], T. Ingebretsen Carlson[45a,45b], G. Introzzi[70a,70b], M. Iodice[74a], V. Ippolito[72a,72b], M. Ishino[150], W. Islam[166], C. Issever[17,46], S. Istin[11c,al], J.M. Iturbe Ponce[62a], R. Iuppa[75a,75b], A. Ivina[165], J.M. Izen[43], V. Izzo[69a], P. Jacka[128], P. Jackson[1], R.M. Jacobs[46], B.P. Jaeger[139], C.S. Jagfeld[106], G. Jäkel[167], K. Jakobs[52], T. Jakoubek[165], J. Jamieson[57], K.W. Janas[82a], G. Jarlskog[95], A.E. Jaspan[89], N. Javadov[36,y], T. Javůrek[34], M. Javurkova[100], F. Jeanneau[132], L. Jeanty[120], J. Jejelava[146a,z], P. Jenni[52,f], S. Jézéquel[4], J. Jia[142], Z. Jia[13c], Y. Jiang[60a], S. Jiggins[50], J. Jimenez Pena[107], S. Jin[13c], A. Jinaru[25b], O. Jinnouchi[151], H. Jivan[31f], P. Johansson[136], K.A. Johns[6], C.A. Johnson[65], D.M. Jones[30], E. Jones[163], R.W.L. Jones[88], T.J. Jones[89], J. Jovicevic[14], X. Ju[16a], J.J. Junggeburth[34], A. Juste Rozas[12,u], S. Kabana[134e], A. Kaczmarska[83], M. Kado[72a,72b], H. Kagan[116], M. Kagan[140], A. Kahn[39], A. Kahn[125], C. Kahra[97], T. Kaji[164], E. Kajomovitz[147], C.W. Kalderon[27], A. Kamenshchikov[35], M. Kaneda[150], N.J. Kang[133], S. Kang[78], Y. Kano[108], D. Kar[31f], K. Karava[123], M.J. Kareem[153b], I. Karkanias[149], S.N. Karpov[36], Z.M. Karpova[36], V. Kartvelishvili[88], A.N. Karyukhin[35], E. Kasimi[149], C. Kato[60d], J. Katzy[46], K. Kawade[137], K. Kawagoe[86], T. Kawaguchi[108], T. Kawamoto[132], G. Kawamura[53], E.F. Kay[161], F.I. Kaya[155], S. Kazakos[12], V.F. Kazanin[35], Y. Ke[142], J.M. Keaveney[31a], R. Keeler[161], J.S. Keller[32], A.S. Kelly[93], D. Kelsey[143], J.J. Kempster[19], J. Kendrick[19], K.E. Kennedy[39], O. Kepka[128], S. Kersten[167], B.P. Kerševan[90], S. Ketabchi Haghighat[152], M. Khandoga[124], A. Khanov[118], A.G. Kharlamov[35], T. Kharlamova[35], E.E. Khoda[135], T.J. Khoo[17], G. Khoriauli[162], J. Khubua[146b], S. Kido[81], M. Kiehn[34], A. Kilgallon[120], E. Kim[151], Y.K. Kim[37], N. Kimura[93], A. Kirchhoff[53], D. Kirchmeier[48], C. Kirfel[22], J. Kirk[131], A.E. Kiryunin[107], T. Kishimoto[150], D.P. Kisliuk[152], C. Kitsaki[9], O. Kivernyk[22],

JHEP07(2023)125

T. Klapdor-Kleingrothaus[52], M. Klassen[61a], C. Klein[32], L. Klein[162], M.H. Klein[103], M. Klein[89], U. Klein[89], P. Klimek[34], A. Klimentov[27], F. Klimpel[107], T. Klingl[22], T. Klioutchnikova[34], F.F. Klitzner[106], P. Kluit[111], S. Kluth[107], E. Kneringer[76], T.M. Knight[152], A. Knue[52], D. Kobayashi[86], R. Kobayashi[84], M. Kobel[48], M. Kocian[140], T. Kodama[150], P. Kodyš[130], D.M. Koeck[143], P.T. Koenig[22], T. Koffas[32], N.M. Köhler[34], M. Kolb[132], I. Koletsou[4], T. Komarek[119], K. Köneke[52], A.X.Y. Kong[1], T. Kono[115], V. Konstantinides[93], N. Konstantinidis[93], B. Konya[95], R. Kopeliansky[65], S. Koperny[82a], K. Korcyl[83], K. Kordas[149], G. Koren[148], A. Korn[93], S. Korn[53], I. Korolkov[12], E.V. Korolkova[136], N. Korotkova[35], B. Kortman[111], O. Kortner[107], S. Kortner[107], W.H. Kostecka[112], V.V. Kostyukhin[138,35], A. Kotsokechagia[64], A. Kotwal[49], A. Koulouris[34], A. Kourkoumeli-Charalampidi[70a,70b], C. Kourkoumelis[8], E. Kourlitis[5], O. Kovanda[143], R. Kowalewski[161], W. Kozanecki[132], A.S. Kozhin[35], V.A. Kramarenko[35], G. Kramberger[90], P. Kramer[97], D. Krasnopevtsev[60a], M.W. Krasny[124], A. Krasznahorkay[34], J.A. Kremer[97], J. Kretzschmar[89], K. Kreul[17], P. Krieger[152], F. Krieter[106], S. Krishnamurthy[100], A. Krishnan[61b], M. Krivos[130], K. Krizka[16a], K. Kroeninger[47], H. Kroha[107], J. Kroll[128], J. Kroll[125], K.S. Krowpman[104], U. Kruchonak[36], H. Krüger[22], N. Krumnack[78], M.C. Kruse[49], J.A. Krzysiak[83], A. Kubota[151], O. Kuchinskaia[35], S. Kuday[3a], D. Kuechler[46], J.T. Kuechler[46], S. Kuehn[34], T. Kuhl[46], V. Kukhtin[36], Y. Kulchitsky[35,a], S. Kuleshov[134d], M. Kumar[31f], N. Kumari[99], M. Kuna[58], A. Kupco[128], T. Kupfer[47], O. Kuprash[52], H. Kurashige[81], L.L. Kurchaninov[153a], Y.A. Kurochkin[35], A. Kurova[35], M.G. Kurth[13a,13d], E.S. Kuwertz[34], M. Kuze[151], A.K. Kvam[135], J. Kvita[119], T. Kwan[101], K.W. Kwok[62a], C. Lacasta[159], F. Lacava[72a,72b], H. Lacker[17], D. Lacour[124], N.N. Lad[93], E. Ladygin[36], R. Lafaye[4], B. Laforge[124], T. Lagouri[134e], S. Lai[53], I.K. Lakomiec[82a], N. Lalloue[58], J.E. Lambert[117], S. Lammers[65], W. Lampl[6], C. Lampoudis[149], E. Lançon[27], U. Landgraf[52], M.P.J. Landon[91], V.S. Lang[52], J.C. Lange[53], R.J. Langenberg[100], A.J. Lankford[156], F. Lanni[27], K. Lantzsch[22], A. Lanza[70a], A. Lapertosa[55b,55a], J.F. Laporte[132], T. Lari[68a], F. Lasagni Manghi[21b], M. Lassnig[34], V. Latonova[128], T.S. Lau[62a], A. Laudrain[97], A. Laurier[32], M. Lavorgna[69a,69b], S.D. Lawlor[92], Z. Lawrence[98], M. Lazzaroni[68a,68b], B. Le[98], B. Leban[90], A. Lebedev[78], M. LeBlanc[34], T. LeCompte[5], F. Ledroit-Guillon[58], A.C.A. Lee[93], G.R. Lee[15], L. Lee[59], S.C. Lee[145], S. Lee[78], L.L. Leeuw[31c], B. Lefebvre[153a], H.P. Lefebvre[92], M. Lefebvre[161], C. Leggett[16a], K. Lehmann[139], N. Lehmann[18], G. Lehmann Miotto[34], W.A. Leight[46], A. Leisos[149,t], M.A.L. Leite[79d], C.E. Leitgeb[46], R. Leitner[130], K.J.C. Leney[42], T. Lenz[22], S. Leone[71a], C. Leonidopoulos[50], A. Leopold[141], C. Leroy[105], R. Les[104], C.G. Lester[30], M. Levchenko[35], J. Levêque[4], D. Levin[103], L.J. Levinson[165], D.J. Lewis[19], B. Li[13b], B. Li[60b], C. Li[60a], C-Q. Li[60c,60d], H. Li[60a], H. Li[60b], H. Li[60b], J. Li[60c], K. Li[135], L. Li[60c], M. Li[13a,13d], Q.Y. Li[60a], S. Li[60d,60c,d], T. Li[60b], X. Li[46], Y. Li[46], Z. Li[60b], Z. Li[123], Z. Li[101], Z. Li[89], Z. Liang[13a], M. Liberatore[46], B. Liberti[73a], K. Lie[62c], J. Lieber Marin[79b], K. Lin[104], R.A. Linck[65], R.E. Lindley[6], J.H. Lindon[2], A. Linss[46], E. Lipeles[125], A. Lipniacka[15], T.M. Liss[158,ag], A. Lister[160], J.D. Little[7], B. Liu[13a], B.X. Liu[139], J.B. Liu[60a], J.K.K. Liu[37], K. Liu[60d,60c],

JHEP07(2023)125

M. Liu[60a], M.Y. Liu[60a], P. Liu[13a], X. Liu[60a], Y. Liu[46], Y. Liu[13c,13d], Y.L. Liu[103], Y.W. Liu[60a], M. Livan[70a,70b], J. Llorente Merino[139], S.L. Lloyd[91], E.M. Lobodzinska[46], P. Loch[6], S. Loffredo[73a,73b], T. Lohse[17], K. Lohwasser[136], M. Lokajicek[128,*], J.D. Long[158], I. Longarini[72a,72b], L. Longo[34], R. Longo[158], I. Lopez Paz[12], A. Lopez Solis[46], J. Lorenz[106], N. Lorenzo Martinez[4], A.M. Lory[106], A. Lösle[52], X. Lou[45a,45b], X. Lou[13a,13d], A. Lounis[64], J. Love[5], P.A. Love[88], J.J. Lozano Bahilo[159], G. Lu[13a,13d], M. Lu[60a], S. Lu[125], Y.J. Lu[63], H.J. Lubatti[135], C. Luci[72a,72b], F.L. Lucio Alves[13c], A. Lucotte[58], F. Luehring[65], I. Luise[142], L. Luminari[72a], O. Lundberg[141], B. Lund-Jensen[141], N.A. Luongo[120], M.S. Lutz[148], D. Lynn[27], H. Lyons[89], R. Lysak[128], E. Lytken[95], F. Lyu[13a], V. Lyubushkin[36], T. Lyubushkina[36], H. Ma[27], L.L. Ma[60b], Y. Ma[93], D.M. Mac Donell[161], G. Maccarrone[51], C.M. Macdonald[136], J.C. MacDonald[136], R. Madar[38], W.F. Mader[48], M. Madugoda Ralalage Don[118], N. Madysa[48], J. Maeda[81], T. Maeno[27], M. Maerker[48], V. Magerl[52], J. Magro[66a,66c], D.J. Mahon[39], C. Maidantchik[79b], A. Maio[127a,127b,127d], K. Maj[82a], O. Majersky[26a], S. Majewski[120], N. Makovec[64], V. Maksimovic[14], B. Malaescu[124], Pa. Malecki[83], V.P. Maleev[35], F. Malek[58], D. Malito[41b,41a], U. Mallik[77], C. Malone[30], S. Maltezos[9], S. Malyukov[36], J. Mamuzic[159], G. Mancini[51], J.P. Mandalia[91], I. Mandić[90], L. Manhaes de Andrade Filho[79a], I.M. Maniatis[149], M. Manisha[132], J. Manjarres Ramos[48], K.H. Mankinen[95], A. Mann[106], A. Manousos[76], B. Mansoulie[132], I. Manthos[149], S. Manzoni[111], A. Marantis[149,t], G. Marchiori[124], M. Marcisovsky[128], L. Marcoccia[73a,73b], C. Marcon[95], M. Marjanovic[117], Z. Marshall[16a], S. Marti-Garcia[159], T.A. Martin[163], V.J. Martin[50], B. Martin dit Latour[15], L. Martinelli[72a,72b], M. Martinez[12,u], P. Martinez Agullo[159], V.I. Martinez Outschoorn[100], S. Martin-Haugh[131], V.S. Martoiu[25b], A.C. Martyniuk[93], A. Marzin[34], S.R. Maschek[107], L. Masetti[97], T. Mashimo[150], J. Masik[98], A.L. Maslennikov[35], L. Massa[21b], P. Massarotti[69a,69b], P. Mastrandrea[71a,71b], A. Mastroberardino[41b,41a], T. Masubuchi[150], D. Matakias[27], T. Mathisen[157], A. Matic[106], N. Matsuzawa[150], J. Maurer[25b], B. Maček[90], D.A. Maximov[35], R. Mazini[145], I. Maznas[149], S.M. Mazza[133], C. Mc Ginn[27], J.P. Mc Gowan[101], S.P. Mc Kee[103], T.G. McCarthy[107], W.P. McCormack[16a], E.F. McDonald[102], A.E. McDougall[111], J.A. Mcfayden[143], G. Mchedlidze[146b], M.A. McKay[42], K.D. McLean[161], S.J. McMahon[131], P.C. McNamara[102], R.A. McPherson[161,x], J.E. Mdhluli[31f], Z.A. Meadows[100], S. Meehan[34], T. Megy[38], S. Mehlhase[106], A. Mehta[89], B. Meirose[43], D. Melini[147], B.R. Mellado Garcia[31f], A.H. Melo[53], F. Meloni[46], A. Melzer[22], E.D. Mendes Gouveia[127a], A.M. Mendes Jacques Da Costa[19], H.Y. Meng[152], L. Meng[34], S. Menke[107], M. Mentink[34], E. Meoni[41b,41a], C. Merlassino[123], P. Mermod[54,*], L. Merola[69a,69b], C. Meroni[68a], G. Merz[103], O. Meshkov[35], J.K.R. Meshreki[138], J. Metcalfe[5], A.S. Mete[5], C. Meyer[65], J-P. Meyer[132], M. Michetti[17], R.P. Middleton[131], L. Mijović[50], G. Mikenberg[165], M. Mikestikova[128], M. Mikuž[90], H. Mildner[136], A. Milic[152], C.D. Milke[42], D.W. Miller[37], L.S. Miller[32], A. Milov[165], D.A. Milstead[45a,45b], T. Min[13c], A.A. Minaenko[35], I.A. Minashvili[146b], L. Mince[57], A.I. Mincer[114], B. Mindur[82a], M. Mineev[36], Y. Minegishi[150], Y. Mino[84], L.M. Mir[12], M. Miralles Lopez[159], M. Mironova[123], T. Mitani[164], V.A. Mitsou[159],

JHEP07(2023)125

M. Mittal[60c], O. Miu[152], P.S. Miyagawa[91], Y. Miyazaki[86], A. Mizukami[80], J.U. Mjörnmark[95], T. Mkrtchyan[61a], M. Mlynarikova[112], T. Moa[45a,45b], S. Mobius[53], K. Mochizuki[105], P. Moder[46], P. Mogg[106], A.F. Mohammed[13a,13d], S. Mohapatra[39], G. Mokgatitswane[31f], B. Mondal[138], S. Mondal[129], K. Mönig[46], E. Monnier[99], L. Monsonis Romero[159], A. Montalbano[139], J. Montejo Berlingen[34], M. Montella[116], F. Monticelli[87], N. Morange[64], A.L. Moreira De Carvalho[127a], M. Moreno Llácer[159], C. Moreno Martinez[12], P. Morettini[55b], S. Morgenstern[163], D. Mori[139], M. Morii[59], M. Morinaga[150], V. Morisbak[122], A.K. Morley[34], A.P. Morris[93], L. Morvaj[34], P. Moschovakos[34], B. Moser[111], M. Mosidze[146b], T. Moskalets[52], P. Moskvitina[110], J. Moss[29,o], E.J.W. Moyse[100], S. Muanza[99], J. Mueller[126], D. Muenstermann[88], R. Müller[18], G.A. Mullier[95], J.J. Mullin[125], D.P. Mungo[68a,68b], J.L. Munoz Martinez[12], F.J. Munoz Sanchez[98], M. Murin[98], P. Murin[26b], W.J. Murray[163,131], A. Murrone[68a,68b], J.M. Muse[117], M. Muškinja[16a], C. Mwewa[27], A.G. Myagkov[35,a], A.J. Myers[7], A.A. Myers[126], G. Myers[65], M. Myska[129], B.P. Nachman[16a], O. Nackenhorst[47], A. Nag[48], K. Nagai[123], K. Nagano[80], J.L. Nagle[27], E. Nagy[99], A.M. Nairz[34], Y. Nakahama[108], K. Nakamura[80], H. Nanjo[121], F. Napolitano[61a], R. Narayan[42], E.A. Narayanan[109], I. Naryshkin[35], M. Naseri[32], C. Nass[22], T. Naumann[46], G. Navarro[20a], J. Navarro-Gonzalez[159], R. Nayak[148], P.Y. Nechaeva[35], F. Nechansky[46], T.J. Neep[19], A. Negri[70a,70b], M. Negrini[21b], C. Nellist[110], C. Nelson[101], K. Nelson[103], S. Nemecek[128], M. Nessi[34,g], M.S. Neubauer[158], F. Neuhaus[97], J. Neundorf[46], R. Newhouse[160], P.R. Newman[19], C.W. Ng[126], Y.S. Ng[17], Y.W.Y. Ng[156], B. Ngair[33e], H.D.N. Nguyen[105], R.B. Nickerson[123], R. Nicolaidou[132], D.S. Nielsen[40], J. Nielsen[133], M. Niemeyer[53], N. Nikiforou[10], V. Nikolaenko[35,a], I. Nikolic-Audit[124], K. Nikolopoulos[19], P. Nilsson[27], H.R. Nindhito[54], A. Nisati[72a], N. Nishu[2], R. Nisius[107], T. Nitta[164], T. Nobe[150], D.L. Noel[30], Y. Noguchi[84], I. Nomidis[124], M.A. Nomura[27], M.B. Norfolk[136], R.R.B. Norisam[93], J. Novak[90], T. Novak[46], O. Novgorodova[48], L. Novotny[129], R. Novotny[109], L. Nozka[119], K. Ntekas[156], E. Nurse[93], F.G. Oakham[32,ai], J. Ocariz[124], A. Ochi[81], I. Ochoa[127a], J.P. Ochoa-Ricoux[134a], S. Oda[86], S. Odaka[80], S. Oerdek[157], A. Ogrodnik[82a], A. Oh[98], C.C. Ohm[141], H. Oide[151], R. Oishi[150], M.L. Ojeda[46], Y. Okazaki[84], M.W. O'Keefe[89], Y. Okumura[150], A. Olariu[25b], L.F. Oleiro Seabra[127a], S.A. Olivares Pino[134e], D. Oliveira Damazio[27], D. Oliveira Goncalves[79a], J.L. Oliver[156], M.J.R. Olsson[156], A. Olszewski[83], J. Olszowska[83,*], Ö.O. Öncel[22], D.C. O'Neil[139], A.P. O'Neill[123], A. Onofre[127a,127e], P.U.E. Onyisi[10], R.G. Oreamuno Madriz[112], M.J. Oreglia[37], G.E. Orellana[87], D. Orestano[74a,74b], N. Orlando[12], R.S. Orr[152], V. O'Shea[57], R. Ospanov[60a], G. Otero y Garzon[28], H. Otono[86], P.S. Ott[61a], G.J. Ottino[16a], M. Ouchrif[33d], J. Ouellette[27], F. Ould-Saada[122], A. Ouraou[132,*], Q. Ouyang[13a], M. Owen[57], R.E. Owen[131], K.Y. Oyulmaz[11c], V.E. Ozcan[11c], N. Ozturk[7], S. Ozturk[11c], J. Pacalt[119], H.A. Pacey[30], K. Pachal[49], A. Pacheco Pages[12], C. Padilla Aranda[12], S. Pagan Griso[16a], G. Palacino[65], S. Palazzo[50], S. Palestini[34], M. Palka[82b], P. Palni[82a], D.K. Panchal[10], C.E. Pandini[54], J.G. Panduro Vazquez[92], P. Pani[46], G. Panizzo[66a,66c], L. Paolozzi[54], C. Papadatos[105], S. Parajuli[42], A. Paramonov[5], C. Paraskevopoulos[9], D. Paredes Hernandez[62b], S.R. Paredes Saenz[123],

JHEP07(2023)125

B. Parida[165], T.H. Park[152], A.J. Parker[29], M.A. Parker[30], F. Parodi[55b,55a], E.W. Parrish[112], J.A. Parsons[39], U. Parzefall[52], L. Pascual Dominguez[148], V.R. Pascuzzi[16a], F. Pasquali[111], E. Pasqualucci[72a], S. Passaggio[55b], F. Pastore[92], P. Pasuwan[45a,45b], J.R. Pater[98], A. Pathak[166], J. Patton[89], T. Pauly[34], J. Pearkes[140], M. Pedersen[122], L. Pedraza Diaz[110], R. Pedro[127a], T. Peiffer[53], S.V. Peleganchuk[35], O. Penc[128], C. Peng[62b], H. Peng[60a], M. Penzin[35], B.S. Peralva[79a], A.P. Pereira Peixoto[127a], L. Pereira Sanchez[45a,45b], D.V. Perepelitsa[27], E. Perez Codina[153a], M. Perganti[9], L. Perini[68a,68b,*], H. Pernegger[34], S. Perrella[34], A. Perrevoort[111], K. Peters[46], R.F.Y. Peters[98], B.A. Petersen[34], T.C. Petersen[40], E. Petit[99], V. Petousis[129], C. Petridou[149], P. Petroff[64], F. Petrucci[74a,74b], A. Petrukhin[138], M. Pettee[168], N.E. Pettersson[34], K. Petukhova[130], A. Peyaud[132], R. Pezoa[134f], L. Pezzotti[34], G. Pezzullo[168], T. Pham[102], P.W. Phillips[131], M.W. Phipps[158], G. Piacquadio[142], E. Pianori[16a], F. Piazza[68a,68b], A. Picazio[100], R. Piegaia[28], D. Pietreanu[25b], J.E. Pilcher[37], A.D. Pilkington[98], M. Pinamonti[66a,66c], J.L. Pinfold[2], C. Pitman Donaldson[93], D.A. Pizzi[32], L. Pizzimento[73a,73b], A. Pizzini[111], M.-A. Pleier[27], V. Plesanovs[52], V. Pleskot[130], E. Plotnikova[36], P. Podberezko[35], R. Poettgen[95], R. Poggi[54], L. Poggioli[124], I. Pogrebnyak[104], D. Pohl[22], I. Pokharel[53], G. Polesello[70a], A. Poley[139,153a], A. Policicchio[72a,72b], R. Polifka[130], A. Polini[21b], C.S. Pollard[123], Z.B. Pollock[116], V. Polychronakos[27], D. Ponomarenko[35], L. Pontecorvo[34], S. Popa[25a], G.A. Popeneciu[25d], L. Portales[4], D.M. Portillo Quintero[153a], S. Pospisil[129], P. Postolache[25c], K. Potamianos[123], I.N. Potrap[36], C.J. Potter[30], H. Potti[1], T. Poulsen[46], J. Poveda[159], T.D. Powell[136], G. Pownall[46], M.E. Pozo Astigarraga[34], A. Prades Ibanez[159], P. Pralavorio[99], M.M. Prapa[44], S. Prell[78], D. Price[98], M. Primavera[67a], M.A. Principe Martin[96], M.L. Proffitt[135], N. Proklova[35], K. Prokofiev[62c], S. Protopopescu[27], J. Proudfoot[5], M. Przybycien[82a], D. Pudzha[35], P. Puzo[64], D. Pyatiizbyantseva[35], J. Qian[103], Y. Qin[98], T. Qiu[91], A. Quadt[53], M. Queitsch-Maitland[34], G. Rabanal Bolanos[59], F. Ragusa[68a,68b], J.A. Raine[54], S. Rajagopalan[27], K. Ran[13a,13d], D.F. Rassloff[61a], D.M. Rauch[46], S. Rave[97], B. Ravina[57], I. Ravinovich[165], M. Raymond[34], A.L. Read[122], N.P. Readioff[136], D.M. Rebuzzi[70a,70b], G. Redlinger[27], K. Reeves[43], D. Reikher[148], A. Reiss[97], A. Rej[138], C. Rembser[34], A. Renardi[46], M. Renda[25b], M.B. Rendel[107], A.G. Rennie[57], S. Resconi[68a], M. Ressegotti[55b,55a], E.D. Resseguie[16a], S. Rettie[93], B. Reynolds[116], E. Reynolds[19], M. Rezaei Estabragh[167], O.L. Rezanova[35], P. Reznicek[130], E. Ricci[75a,75b], R. Richter[107], S. Richter[46], E. Richter-Was[82b], M. Ridel[124], P. Rieck[107], P. Riedler[34], O. Rifki[46], M. Rijssenbeek[142], A. Rimoldi[70a,70b], M. Rimoldi[46], L. Rinaldi[21b,21a], T.T. Rinn[158], M.P. Rinnagel[106], G. Ripellino[141], I. Riu[12], P. Rivadeneira[46], J.C. Rivera Vergara[161], F. Rizatdinova[118], E. Rizvi[91], C. Rizzi[54], B.A. Roberts[163], B.R. Roberts[16a], S.H. Robertson[101,x], M. Robin[46], D. Robinson[30], C.M. Robles Gajardo[134f], M. Robles Manzano[97], A. Robson[57], A. Rocchi[73a,73b], C. Roda[71a,71b], S. Rodriguez Bosca[61a], A. Rodriguez Rodriguez[52], A.M. Rodríguez Vera[153b], S. Roe[34], A.R. Roepe-Gier[117], J. Roggel[167], O. Røhne[122], R.A. Rojas[161], B. Roland[52], C.P.A. Roland[65], J. Roloff[27], A. Romaniouk[35], M. Romano[21b], A.C. Romero Hernandez[158], N. Rompotis[89],

JHEP07(2023)125

M. Ronzani[114], L. Roos[124], S. Rosati[72a], B.J. Rosser[125], E. Rossi[152], E. Rossi[4], E. Rossi[69a,69b], L.P. Rossi[55b], L. Rossini[46], R. Rosten[116], M. Rotaru[25b], B. Rottler[52], D. Rousseau[64], D. Rousso[30], G. Rovelli[70a,70b], A. Roy[10], A. Rozanov[99], Y. Rozen[147], X. Ruan[31f], A.J. Ruby[89], T.A. Ruggeri[1], F. Rühr[52], A. Ruiz-Martinez[159], A. Rummler[34], Z. Rurikova[52], N.A. Rusakovich[36], H.L. Russell[34], L. Rustige[38], J.P. Rutherfoord[6], E.M. Rüttinger[136], M. Rybar[130], E.B. Rye[122], A. Ryzhov[35], J.A. Sabater Iglesias[46], P. Sabatini[159], L. Sabetta[72a,72b], H.F-W. Sadrozinski[133], F. Safai Tehrani[72a], B. Safarzadeh Samani[143], M. Safdari[140], S. Saha[101], M. Sahinsoy[107], A. Sahu[167], M. Saimpert[132], M. Saito[150], T. Saito[150], D. Salamani[34], G. Salamanna[74a,74b], A. Salnikov[140], J. Salt[159], A. Salvador Salas[12], D. Salvatore[41b,41a], F. Salvatore[143], A. Salzburger[34], D. Sammel[52], D. Sampsonidis[149], D. Sampsonidou[60d,60c], J. Sánchez[159], A. Sanchez Pineda[4], V. Sanchez Sebastian[159], H. Sandaker[122], C.O. Sander[46], I.G. Sanderswood[88], J.A. Sandesara[100], M. Sandhoff[167], C. Sandoval[20b], D.P.C. Sankey[131], M. Sannino[55b,55a], A. Sansoni[51], C. Santoni[38], H. Santos[127a,127b], S.N. Santpur[16a], A. Santra[165], K.A. Saoucha[136], J.G. Saraiva[127a,127d], J. Sardain[99], O. Sasaki[80], K. Sato[154], C. Sauer[61b], F. Sauerburger[52], E. Sauvan[4], P. Savard[152,ai], R. Sawada[150], C. Sawyer[131], L. Sawyer[94], I. Sayago Galvan[159], C. Sbarra[21b], A. Sbrizzi[21b,21a], T. Scanlon[93], J. Schaarschmidt[135], P. Schacht[107], D. Schaefer[37], U. Schäfer[97], A.C. Schaffer[64], D. Schaile[106], R.D. Schamberger[142], E. Schanet[106], C. Scharf[17], N. Scharmberg[98], V.A. Schegelsky[35], D. Scheirich[130], F. Schenck[17], M. Schernau[156], C. Schiavi[55b,55a], L.K. Schildgen[22], Z.M. Schillaci[24], E.J. Schioppa[67a,67b], M. Schioppa[41b,41a], B. Schlag[97], K.E. Schleicher[52], S. Schlenker[34], K. Schmieden[97], C. Schmitt[97], S. Schmitt[46], L. Schoeffel[132], A. Schoening[61b], P.G. Scholer[52], E. Schopf[123], M. Schott[97], J. Schovancova[34], S. Schramm[54], F. Schroeder[167], H-C. Schultz-Coulon[61a], M. Schumacher[52], B.A. Schumm[133], Ph. Schune[132], A. Schwartzman[140], T.A. Schwarz[103], Ph. Schwemling[132], R. Schwienhorst[104], A. Sciandra[133], G. Sciolla[24], F. Scuri[71a], F. Scutti[102], C.D. Sebastiani[89], K. Sedlaczek[47], P. Seema[17], S.C. Seidel[109], A. Seiden[133], B.D. Seidlitz[27], T. Seiss[37], C. Seitz[46], J.M. Seixas[79b], G. Sekhniaidze[69a], S.J. Sekula[42], L. Selem[4], N. Semprini-Cesari[21b,21a], S. Sen[49], C. Serfon[27], L. Serin[64], L. Serkin[66a,66b], M. Sessa[74a,74b], H. Severini[117], S. Sevova[140], F. Sforza[55b,55a], A. Sfyrla[54], E. Shabalina[53], R. Shaheen[141], J.D. Shahinian[125], N.W. Shaikh[45a,45b], D. Shaked Renous[165], L.Y. Shan[13a], M. Shapiro[16a], A. Sharma[34], A.S. Sharma[1], S. Sharma[46], P.B. Shatalov[35], K. Shaw[143], S.M. Shaw[98], P. Sherwood[93], L. Shi[93], C.O. Shimmin[168], Y. Shimogama[164], J.D. Shinner[92], I.P.J. Shipsey[123], S. Shirabe[54], M. Shiyakova[36,am], J. Shlomi[165], M.J. Shochet[37], J. Shojaii[102], D.R. Shope[141], S. Shrestha[116], E.M. Shrif[31f], M.J. Shroff[161], E. Shulga[165], P. Sicho[128], A.M. Sickles[158], E. Sideras Haddad[31f], O. Sidiropoulou[34], A. Sidoti[21b], F. Siegert[48], Dj. Sijacki[14], J.M. Silva[19], M.V. Silva Oliveira[34], S.B. Silverstein[45a], S. Simion[64], R. Simoniello[34], N.D. Simpson[95], S. Simsek[11b], P. Sinervo[152], V. Sinetckii[35], S. Singh[139], S. Singh[152], S. Sinha[46], S. Sinha[31f], M. Sioli[21b,21a], I. Siral[120], S.Yu. Sivoklokov[35,*], J. Sjölin[45a,45b], A. Skaf[53], E. Skorda[95], P. Skubic[117], M. Slawinska[83], K. Sliwa[155], V. Smakhtin[165], B.H. Smart[131],

JHEP07(2023)125

J. Smiesko[130], S.Yu. Smirnov[35], Y. Smirnov[35], L.N. Smirnova[35,a], O. Smirnova[95], E.A. Smith[37], H.A. Smith[123], M. Smizanska[88], K. Smolek[129], A. Smykiewicz[83], A.A. Snesarev[35], H.L. Snoek[111], S. Snyder[27], R. Sobie[161,x], A. Soffer[148], F. Sohns[53], C.A. Solans Sanchez[34], E.Yu. Soldatov[35], U. Soldevila[159], A.A. Solodkov[35], S. Solomon[52], A. Soloshenko[36], O.V. Solovyanov[35], V. Solovyev[35], P. Sommer[136], H. Son[155], A. Sonay[12], W.Y. Song[153b], A. Sopczak[129], A.L. Sopio[93], F. Sopkova[26b], S. Sottocornola[70a,70b], R. Soualah[66a,66c], Z. Soumaimi[33e], D. South[46], S. Spagnolo[67a,67b], M. Spalla[107], M. Spangenberg[163], F. Spanò[92], D. Sperlich[52], T.M. Spieker[61a], G. Spigo[34], M. Spina[143], D.P. Spiteri[57], M. Spousta[130], A. Stabile[68a,68b], R. Stamen[61a], M. Stamenkovic[111], A. Stampekis[19], M. Standke[22], E. Stanecka[83], B. Stanislaus[34], M.M. Stanitzki[46], M. Stankaityte[123], B. Stapf[46], E.A. Starchenko[35], G.H. Stark[133], J. Stark[99,ac], D.M. Starko[153b], P. Staroba[128], P. Starovoitov[61a], S. Stärz[101], R. Staszewski[83], G. Stavropoulos[44], P. Steinberg[27], A.L. Steinhebel[120], B. Stelzer[139,153a], H.J. Stelzer[126], O. Stelzer-Chilton[153a], H. Stenzel[56], T.J. Stevenson[143], G.A. Stewart[34], M.C. Stockton[34], G. Stoicea[25b], M. Stolarski[127a], S. Stonjek[107], A. Straessner[48], J. Strandberg[141], S. Strandberg[45a,45b], M. Strauss[117], T. Strebler[99], P. Strizenec[26b], R. Ströhmer[162], D.M. Strom[120], L.R. Strom[46], R. Stroynowski[42], A. Strubig[45a,45b], S.A. Stucci[27], B. Stugu[15], J. Stupak[117], N.A. Styles[46], D. Su[140], S. Su[60a], W. Su[60d,135,60c], X. Su[60a], K. Sugizaki[150], V.V. Sulin[35], M.J. Sullivan[89], D.M.S. Sultan[54], L. Sultanaliyeva[35], S. Sultansoy[3c], T. Sumida[84], S. Sun[103], S. Sun[166], X. Sun[98], O. Sunneborn Gudnadottir[157], C.J.E. Suster[144], M.R. Sutton[143], M. Svatos[128], M. Swiatlowski[153a], T. Swirski[162], I. Sykora[26a], M. Sykora[130], T. Sykora[130], D. Ta[97], K. Tackmann[46,v], A. Taffard[156], R. Tafirout[153a], R.H.M. Taibah[124], R. Takashima[85], K. Takeda[81], T. Takeshita[137], E.P. Takeva[50], Y. Takubo[80], M. Talby[99], A.A. Talyshev[35], K.C. Tam[62b], N.M. Tamir[148], A. Tanaka[150], J. Tanaka[150], R. Tanaka[64], J. Tang[60c], Z. Tao[160], S. Tapia Araya[78], S. Tapprogge[97], A. Tarek Abouelfadl Mohamed[104], S. Tarem[147], K. Tariq[60b], G. Tarna[25b], G.F. Tartarelli[68a], P. Tas[130], M. Tasevsky[128], E. Tassi[41b,41a], G. Tateno[150], Y. Tayalati[33e], G.N. Taylor[102], W. Taylor[153b], H. Teagle[89], A.S. Tee[166], R. Teixeira De Lima[140], P. Teixeira-Dias[92], H. Ten Kate[34], J.J. Teoh[111], K. Terashi[150], J. Terron[96], S. Terzo[12], M. Testa[51], R.J. Teuscher[152,x], N. Themistokleous[50], T. Theveneaux-Pelzer[17], O. Thielmann[167], D.W. Thomas[92], J.P. Thomas[19], E.A. Thompson[46], P.D. Thompson[19], E. Thomson[125], E.J. Thorpe[91], Y. Tian[53], V. Tikhomirov[35,a], Yu.A. Tikhonov[35], S. Timoshenko[35], P. Tipton[168], S. Tisserant[99], S.H. Tlou[31f], A. Tnourji[38], K. Todome[21b,21a], S. Todorova-Nova[130], S. Todt[48], M. Togawa[80], J. Tojo[86], S. Tokár[26a], K. Tokushuku[80], E. Tolley[116], R. Tombs[30], M. Tomoto[80,108], L. Tompkins[140,q], P. Tornambe[100], E. Torrence[120], H. Torres[48], E. Torró Pastor[159], M. Toscani[28], C. Tosciri[37], J. Toth[99,w], D.R. Tovey[136], A. Traeet[15], C.J. Treado[114], T. Trefzger[162], A. Tricoli[27], I.M. Trigger[153a], S. Trincaz-Duvoid[124], D.A. Trischuk[160], B. Trocmé[58], A. Trofymov[64], C. Troncon[68a], F. Trovato[143], L. Truong[31c], M. Trzebinski[83], A. Trzupek[83], F. Tsai[142], A. Tsiamis[149], P.V. Tsiareshka[35,a], A. Tsirigotis[149,t], V. Tsiskaridze[142], E.G. Tskhadadze[146a],

JHEP07(2023)125

M. Tsopoulou[149], Y. Tsujikawa[84], I.I. Tsukerman[35], V. Tsulaia[16a], S. Tsuno[80], O. Tsur[147], D. Tsybychev[142], Y. Tu[62b], A. Tudorache[25b], V. Tudorache[25b], A.N. Tuna[34], S. Turchikhin[36], I. Turk Cakir[3a], R.J. Turner[19], R. Turra[68a], P.M. Tuts[39], S. Tzamarias[149], P. Tzanis[9], E. Tzovara[97], K. Uchida[150], F. Ukegawa[154], P.A. Ulloa Poblete[134d], G. Unal[34], M. Unal[10], A. Undrus[27], G. Unel[156], F.C. Ungaro[102], K. Uno[150], J. Urban[26b], P. Urquijo[102], G. Usai[7], R. Ushioda[151], M. Usman[105], Z. Uysal[11d], V. Vacek[129], B. Vachon[101], K.O.H. Vadla[122], T. Vafeiadis[34], C. Valderanis[106], E. Valdes Santurio[45a,45b], M. Valente[153a], S. Valentinetti[21b,21a], A. Valero[159], R.A. Vallance[19], A. Vallier[99,ac], J.A. Valls Ferrer[159], T.R. Van Daalen[135], P. Van Gemmeren[5], S. Van Stroud[93], I. Van Vulpen[111], M. Vanadia[73a,73b], W. Vandelli[34], M. Vandenbroucke[132], E.R. Vandewall[118], D. Vannicola[148], L. Vannoli[55b,55a], R. Vari[72a], E.W. Varnes[6], C. Varni[16a], T. Varol[145], D. Varouchas[64], K.E. Varvell[144], M.E. Vasile[25b], L. Vaslin[38], G.A. Vasquez[161], F. Vazeille[38], D. Vazquez Furelos[12], T. Vazquez Schroeder[34], J. Veatch[53], V. Vecchio[98], M.J. Veen[111], I. Veliscek[123], L.M. Veloce[152], F. Veloso[127a,127c], S. Veneziano[72a], A. Ventura[67a,67b], A. Verbytskyi[107], M. Verducci[71a,71b], C. Vergis[22], M. Verissimo De Araujo[79b], W. Verkerke[111], A.T. Vermeulen[111], J.C. Vermeulen[111], C. Vernieri[140], P.J. Verschuuren[92], M. Vessella[100], M.L. Vesterbacka[114], M.C. Vetterli[139,ai], A. Vgenopoulos[149], N. Viaux Maira[134f], T. Vickey[136], O.E. Vickey Boeriu[136], G.H.A. Viehhauser[123], L. Vigani[61b], M. Villa[21b,21a], M. Villaplana Perez[159], E.M. Villhauer[50], E. Vilucchi[51], M.G. Vincter[32], G.S. Virdee[19], A. Vishwakarma[50], C. Vittori[21b,21a], I. Vivarelli[143], V. Vladimirov[163], E. Voevodina[107], M. Vogel[167], P. Vokac[129], J. Von Ahnen[46], E. Von Toerne[22], V. Vorobel[130], K. Vorobev[35], M. Vos[159], J.H. Vossebeld[89], M. Vozak[98], L. Vozdecky[91], N. Vranjes[14], M. Vranjes Milosavljevic[14], V. Vrba[129,*], M. Vreeswijk[111], R. Vuillermet[34], O. Vujinovic[97], I. Vukotic[37], S. Wada[154], C. Wagner[100], W. Wagner[167], S. Wahdan[167], H. Wahlberg[87], R. Wakasa[154], M. Wakida[108], V.M. Walbrecht[107], J. Walder[131], R. Walker[106], S.D. Walker[92], W. Walkowiak[138], A.M. Wang[59], A.Z. Wang[166], C. Wang[60a], C. Wang[60c], H. Wang[16a], J. Wang[62a], P. Wang[42], R.-J. Wang[97], R. Wang[59], R. Wang[112], S.M. Wang[145], S. Wang[60b], T. Wang[60a], W.T. Wang[77], W.X. Wang[60a], X. Wang[13c], X. Wang[158], X. Wang[60c], Y. Wang[60a], Z. Wang[103], C. Wanotayaroj[34], A. Warburton[101], C.P. Ward[30], R.J. Ward[19], N. Warrack[57], A.T. Watson[19], M.F. Watson[19], G. Watts[135], B.M. Waugh[93], A.F. Webb[10], C. Weber[27], M.S. Weber[18], S.A. Weber[32], S.M. Weber[61a], C. Wei[60a], Y. Wei[123], A.R. Weidberg[123], J. Weingarten[47], M. Weirich[97], C. Weiser[52], T. Wenaus[27], B. Wendland[47], T. Wengler[34], S. Wenig[34], N. Wermes[22], M. Wessels[61a], K. Whalen[120], A.M. Wharton[88], A.S. White[59], A. White[7], M.J. White[1], D. Whiteson[156], L. Wickremasinghe[121], W. Wiedenmann[166], C. Wiel[48], M. Wielers[131], N. Wieseotte[97], C. Wiglesworth[40], L.A.M. Wiik-Fuchs[52], D.J. Wilbern[117], H.G. Wilkens[34], L.J. Wilkins[92], D.M. Williams[39], H.H. Williams[125], S. Williams[30], S. Willocq[100], P.J. Windischhofer[123], I. Wingerter-Seez[4], F. Winklmeier[120], B.T. Winter[52], M. Wittgen[140], M. Wobisch[94], A. Wolf[97], R. Wölker[123], J. Wollrath[156], M.W. Wolter[83],

JHEP07(2023)125

H. Wolters[127a,127c], V.W.S. Wong[160], A.F. Wongel[46], S.D. Worm[46], B.K. Wosiek[83], K.W. Woźniak[83], K. Wraight[57], J. Wu[13a,13d], S.L. Wu[166], X. Wu[54], Y. Wu[60a], Z. Wu[132,60a], J. Wuerzinger[123], T.R. Wyatt[98], B.M. Wynne[50], S. Xella[40], L. Xia[13c], M. Xia[13b], J. Xiang[62c], X. Xiao[103], M. Xie[60a], X. Xie[60a], I. Xiotidis[143], D. Xu[13a], H. Xu[60a], H. Xu[60a], L. Xu[60a], R. Xu[125], T. Xu[60a], W. Xu[103], Y. Xu[13b], Z. Xu[60b], Z. Xu[140], B. Yabsley[144], S. Yacoob[31a], N. Yamaguchi[86], Y. Yamaguchi[151], M. Yamatani[150], H. Yamauchi[154], T. Yamazaki[16a], Y. Yamazaki[81], J. Yan[60c], S. Yan[123], Z. Yan[23], H.J. Yang[60c,60d], H.T. Yang[16a], S. Yang[60a], T. Yang[62c], X. Yang[60a], X. Yang[13a], Y. Yang[150], Z. Yang[60a,103], W-M. Yao[16a], Y.C. Yap[46], H. Ye[13c], J. Ye[42], S. Ye[27], I. Yeletskikh[36], M.R. Yexley[88], P. Yin[39], K. Yorita[164], K. Yoshihara[78], C.J.S. Young[52], C. Young[140], M. Yuan[103], R. Yuan[60b,j], X. Yue[61a], M. Zaazoua[33e], B. Zabinski[83], G. Zacharis[9], E. Zaid[50], T. Zakareishvili[146b], N. Zakharchuk[32], S. Zambito[34], D. Zanzi[52], S.V. Zeißner[47], C. Zeitnitz[167], J.C. Zeng[158], D.T. Zenger Jr[24], O. Zenin[35], T. Ženiš[26a], S. Zenz[91], S. Zerradi[33a], D. Zerwas[64], B. Zhang[13c], D.F. Zhang[136], G. Zhang[13b], J. Zhang[5], K. Zhang[13a,13d], L. Zhang[13c], M. Zhang[158], R. Zhang[166], S. Zhang[103], X. Zhang[60c], X. Zhang[60b], Z. Zhang[64], P. Zhao[49], T. Zhao[60b], Y. Zhao[133], Z. Zhao[60a], A. Zhemchugov[36], Z. Zheng[140], D. Zhong[158], B. Zhou[103], C. Zhou[166], H. Zhou[6], N. Zhou[60c], Y. Zhou[6], C.G. Zhu[60b], C. Zhu[13a,13d], H.L. Zhu[60a], H. Zhu[13a], J. Zhu[103], Y. Zhu[60a], X. Zhuang[13a], K. Zhukov[35], V. Zhulanov[35], D. Zieminska[65], N.I. Zimine[36], S. Zimmermann[52,*], J. Zinsser[61b], M. Ziolkowski[138], L. Živković[14], A. Zoccoli[21b,21a], K. Zoch[54], T.G. Zorbas[136], O. Zormpa[44], W. Zou[39], L. Zwalinski[34]

[1] *Department of Physics, University of Adelaide, Adelaide; Australia*
[2] *Department of Physics, University of Alberta, Edmonton AB; Canada*
[3] [(a)] *Department of Physics, Ankara University, Ankara;* [(b)] *Istanbul Aydin University, Application and Research Center for Advanced Studies, Istanbul;* [(c)] *Division of Physics, TOBB University of Economics and Technology, Ankara; Türkiye*
[4] *LAPP, Université Savoie Mont Blanc, CNRS/IN2P3, Annecy; France*
[5] *High Energy Physics Division, Argonne National Laboratory, Argonne IL; United States of America*
[6] *Department of Physics, University of Arizona, Tucson AZ; United States of America*
[7] *Department of Physics, University of Texas at Arlington, Arlington TX; United States of America*
[8] *Physics Department, National and Kapodistrian University of Athens, Athens; Greece*
[9] *Physics Department, National Technical University of Athens, Zografou; Greece*
[10] *Department of Physics, University of Texas at Austin, Austin TX; United States of America*
[11] [(a)] *Bahcesehir University, Faculty of Engineering and Natural Sciences, Istanbul;* [(b)] *Istanbul Bilgi University, Faculty of Engineering and Natural Sciences, Istanbul;* [(c)] *Department of Physics, Bogazici University, Istanbul;* [(d)] *Department of Physics Engineering, Gaziantep University, Gaziantep; Türkiye*
[12] *Institut de Física d'Altes Energies (IFAE), Barcelona Institute of Science and Technology, Barcelona; Spain*
[13] [(a)] *Institute of High Energy Physics, Chinese Academy of Sciences, Beijing;* [(b)] *Physics Department, Tsinghua University, Beijing;* [(c)] *Department of Physics, Nanjing University, Nanjing;* [(d)] *University of Chinese Academy of Science (UCAS), Beijing; China*
[14] *Institute of Physics, University of Belgrade, Belgrade; Serbia*
[15] *Department for Physics and Technology, University of Bergen, Bergen; Norway*
[16] [(a)] *Physics Division, Lawrence Berkeley National Laboratory, Berkeley CA;* [(b)] *University of California, Berkeley CA; United States of America*
[17] *Institut für Physik, Humboldt Universität zu Berlin, Berlin; Germany*

JHEP07(2023)125

[18] Albert Einstein Center for Fundamental Physics and Laboratory for High Energy Physics, University of Bern, Bern; Switzerland
[19] School of Physics and Astronomy, University of Birmingham, Birmingham; United Kingdom
[20] [(a)] Facultad de Ciencias y Centro de Investigaciónes, Universidad Antonio Nariño, Bogotá;[(b)] Departamento de Física, Universidad Nacional de Colombia, Bogotá; Colombia
[21] [(a)] Dipartimento di Fisica e Astronomia A. Righi, Università di Bologna, Bologna;[(b)] INFN Sezione di Bologna; Italy
[22] Physikalisches Institut, Universität Bonn, Bonn; Germany
[23] Department of Physics, Boston University, Boston MA; United States of America
[24] Department of Physics, Brandeis University, Waltham MA; United States of America
[25] [(a)] Transilvania University of Brasov, Brasov;[(b)] Horia Hulubei National Institute of Physics and Nuclear Engineering, Bucharest;[(c)] Department of Physics, Alexandru Ioan Cuza University of Iasi, Iasi;[(d)] National Institute for Research and Development of Isotopic and Molecular Technologies, Physics Department, Cluj-Napoca;[(e)] University Politehnica Bucharest, Bucharest;[(f)] West University in Timisoara, Timisoara; Romania
[26] [(a)] Faculty of Mathematics, Physics and Informatics, Comenius University, Bratislava;[(b)] Department of Subnuclear Physics, Institute of Experimental Physics of the Slovak Academy of Sciences, Kosice; Slovak Republic
[27] Physics Department, Brookhaven National Laboratory, Upton NY; United States of America
[28] Universidad de Buenos Aires, Facultad de Ciencias Exactas y Naturales, Departamento de Física, y CONICET, Instituto de Física de Buenos Aires (IFIBA), Buenos Aires; Argentina
[29] California State University, CA; United States of America
[30] Cavendish Laboratory, University of Cambridge, Cambridge; United Kingdom
[31] [(a)] Department of Physics, University of Cape Town, Cape Town;[(b)] iThemba Labs, Western Cape;[(c)] Department of Mechanical Engineering Science, University of Johannesburg, Johannesburg;[(d)] National Institute of Physics, University of the Philippines Diliman (Philippines);[(e)] University of South Africa, Department of Physics, Pretoria;[(f)] School of Physics, University of the Witwatersrand, Johannesburg; South Africa
[32] Department of Physics, Carleton University, Ottawa ON; Canada
[33] [(a)] Faculté des Sciences Ain Chock, Réseau Universitaire de Physique des Hautes Energies — Université Hassan II, Casablanca;[(b)] Faculté des Sciences, Université Ibn-Tofail, Kénitra;[(c)] Faculté des Sciences Semlalia, Université Cadi Ayyad, LPHEA-Marrakech;[(d)] LPMR, Faculté des Sciences, Université Mohamed Premier, Oujda;[(e)] Faculté des sciences, Université Mohammed V, Rabat;[(f)] Institute of Applied Physics, Mohammed VI Polytechnic University, Ben Guerir; Morocco
[34] CERN, Geneva; Switzerland
[35] Affiliated with an institute covered by a cooperation agreement with CERN
[36] Affiliated with an international laboratory covered by a cooperation agreement with CERN
[37] Enrico Fermi Institute, University of Chicago, Chicago IL; United States of America
[38] LPC, Université Clermont Auvergne, CNRS/IN2P3, Clermont-Ferrand; France
[39] Nevis Laboratory, Columbia University, Irvington NY; United States of America
[40] Niels Bohr Institute, University of Copenhagen, Copenhagen; Denmark
[41] [(a)] Dipartimento di Fisica, Università della Calabria, Rende;[(b)] INFN Gruppo Collegato di Cosenza, Laboratori Nazionali di Frascati; Italy
[42] Physics Department, Southern Methodist University, Dallas TX; United States of America
[43] Physics Department, University of Texas at Dallas, Richardson TX; United States of America
[44] National Centre for Scientific Research "Demokritos", Agia Paraskevi; Greece
[45] [(a)] Department of Physics, Stockholm University;[(b)] Oskar Klein Centre, Stockholm; Sweden
[46] Deutsches Elektronen-Synchrotron DESY, Hamburg and Zeuthen; Germany
[47] Fakultät Physik , Technische Universität Dortmund, Dortmund; Germany
[48] Institut für Kern- und Teilchenphysik, Technische Universität Dresden, Dresden; Germany
[49] Department of Physics, Duke University, Durham NC; United States of America
[50] SUPA — School of Physics and Astronomy, University of Edinburgh, Edinburgh; United Kingdom

JHEP07(2023)125

[51] INFN e Laboratori Nazionali di Frascati, Frascati; Italy
[52] Physikalisches Institut, Albert-Ludwigs-Universität Freiburg, Freiburg; Germany
[53] II. Physikalisches Institut, Georg-August-Universität Göttingen, Göttingen; Germany
[54] Département de Physique Nucléaire et Corpusculaire, Université de Genève, Genève; Switzerland
[55] [(a)] Dipartimento di Fisica, Università di Genova, Genova;[(b)] INFN Sezione di Genova; Italy
[56] II. Physikalisches Institut, Justus-Liebig-Universität Giessen, Giessen; Germany
[57] SUPA — School of Physics and Astronomy, University of Glasgow, Glasgow; United Kingdom
[58] LPSC, Université Grenoble Alpes, CNRS/IN2P3, Grenoble INP, Grenoble; France
[59] Laboratory for Particle Physics and Cosmology, Harvard University, Cambridge MA; United States of America
[60] [(a)] Department of Modern Physics and State Key Laboratory of Particle Detection and Electronics, University of Science and Technology of China, Hefei;[(b)] Institute of Frontier and Interdisciplinary Science and Key Laboratory of Particle Physics and Particle Irradiation (MOE), Shandong University, Qingdao;[(c)] School of Physics and Astronomy, Shanghai Jiao Tong University, Key Laboratory for Particle Astrophysics and Cosmology (MOE), SKLPPC, Shanghai;[(d)] Tsung-Dao Lee Institute, Shanghai; China
[61] [(a)] Kirchhoff-Institut für Physik, Ruprecht-Karls-Universität Heidelberg, Heidelberg;[(b)] Physikalisches Institut, Ruprecht-Karls-Universität Heidelberg, Heidelberg; Germany
[62] [(a)] Department of Physics, Chinese University of Hong Kong, Shatin, N.T., Hong Kong;[(b)] Department of Physics, University of Hong Kong, Hong Kong;[(c)] Department of Physics and Institute for Advanced Study, Hong Kong University of Science and Technology, Clear Water Bay, Kowloon, Hong Kong; China
[63] Department of Physics, National Tsing Hua University, Hsinchu; Taiwan
[64] IJCLab, Université Paris-Saclay, CNRS/IN2P3, 91405, Orsay; France
[65] Department of Physics, Indiana University, Bloomington IN; United States of America
[66] [(a)] INFN Gruppo Collegato di Udine, Sezione di Trieste, Udine;[(b)] ICTP, Trieste;[(c)] Dipartimento Politecnico di Ingegneria e Architettura, Università di Udine, Udine; Italy
[67] [(a)] INFN Sezione di Lecce;[(b)] Dipartimento di Matematica e Fisica, Università del Salento, Lecce; Italy
[68] [(a)] INFN Sezione di Milano;[(b)] Dipartimento di Fisica, Università di Milano, Milano; Italy
[69] [(a)] INFN Sezione di Napoli;[(b)] Dipartimento di Fisica, Università di Napoli, Napoli; Italy
[70] [(a)] INFN Sezione di Pavia;[(b)] Dipartimento di Fisica, Università di Pavia, Pavia; Italy
[71] [(a)] INFN Sezione di Pisa;[(b)] Dipartimento di Fisica E. Fermi, Università di Pisa, Pisa; Italy
[72] [(a)] INFN Sezione di Roma;[(b)] Dipartimento di Fisica, Sapienza Università di Roma, Roma; Italy
[73] [(a)] INFN Sezione di Roma Tor Vergata;[(b)] Dipartimento di Fisica, Università di Roma Tor Vergata, Roma; Italy
[74] [(a)] INFN Sezione di Roma Tre;[(b)] Dipartimento di Matematica e Fisica, Università Roma Tre, Roma; Italy
[75] [(a)] INFN-TIFPA;[(b)] Università degli Studi di Trento, Trento; Italy
[76] Universität Innsbruck, Department of Astro and Particle Physics, Innsbruck; Austria
[77] University of Iowa, Iowa City IA; United States of America
[78] Department of Physics and Astronomy, Iowa State University, Ames IA; United States of America
[79] [(a)] Departamento de Engenharia Elétrica, Universidade Federal de Juiz de Fora (UFJF), Juiz de Fora;[(b)] Universidade Federal do Rio De Janeiro COPPE/EE/IF, Rio de Janeiro;[(c)] Universidade Federal de São João del Rei (UFSJ), São João del Rei;[(d)] Instituto de Física, Universidade de São Paulo, São Paulo; Brazil
[80] KEK, High Energy Accelerator Research Organization, Tsukuba; Japan
[81] Graduate School of Science, Kobe University, Kobe; Japan
[82] [(a)] AGH University of Science and Technology, Faculty of Physics and Applied Computer Science, Krakow;[(b)] Marian Smoluchowski Institute of Physics, Jagiellonian University, Krakow; Poland
[83] Institute of Nuclear Physics Polish Academy of Sciences, Krakow; Poland
[84] Faculty of Science, Kyoto University, Kyoto; Japan
[85] Kyoto University of Education, Kyoto; Japan

JHEP07(2023)125

[86] Research Center for Advanced Particle Physics and Department of Physics, Kyushu University, Fukuoka; Japan
[87] Instituto de Física La Plata, Universidad Nacional de La Plata and CONICET, La Plata; Argentina
[88] Physics Department, Lancaster University, Lancaster; United Kingdom
[89] Oliver Lodge Laboratory, University of Liverpool, Liverpool; United Kingdom
[90] Department of Experimental Particle Physics, Jožef Stefan Institute and Department of Physics, University of Ljubljana, Ljubljana; Slovenia
[91] School of Physics and Astronomy, Queen Mary University of London, London; United Kingdom
[92] Department of Physics, Royal Holloway University of London, Egham; United Kingdom
[93] Department of Physics and Astronomy, University College London, London; United Kingdom
[94] Louisiana Tech University, Ruston LA; United States of America
[95] Fysiska institutionen, Lunds universitet, Lund; Sweden
[96] Departamento de Física Teorica C-15 and CIAFF, Universidad Autónoma de Madrid, Madrid; Spain
[97] Institut für Physik, Universität Mainz, Mainz; Germany
[98] School of Physics and Astronomy, University of Manchester, Manchester; United Kingdom
[99] CPPM, Aix-Marseille Université, CNRS/IN2P3, Marseille; France
[100] Department of Physics, University of Massachusetts, Amherst MA; United States of America
[101] Department of Physics, McGill University, Montreal QC; Canada
[102] School of Physics, University of Melbourne, Victoria; Australia
[103] Department of Physics, University of Michigan, Ann Arbor MI; United States of America
[104] Department of Physics and Astronomy, Michigan State University, East Lansing MI; United States of America
[105] Group of Particle Physics, University of Montreal, Montreal QC; Canada
[106] Fakultät für Physik, Ludwig-Maximilians-Universität München, München; Germany
[107] Max-Planck-Institut für Physik (Werner-Heisenberg-Institut), München; Germany
[108] Graduate School of Science and Kobayashi-Maskawa Institute, Nagoya University, Nagoya; Japan
[109] Department of Physics and Astronomy, University of New Mexico, Albuquerque NM; United States of America
[110] Institute for Mathematics, Astrophysics and Particle Physics, Radboud University/Nikhef, Nijmegen; Netherlands
[111] Nikhef National Institute for Subatomic Physics and University of Amsterdam, Amsterdam; Netherlands
[112] Department of Physics, Northern Illinois University, DeKalb IL; United States of America
[113] [(a)] New York University Abu Dhabi, Abu Dhabi;[(b)] United Arab Emirates University, Al Ain;[(c)] University of Sharjah, Sharjah; United Arab Emirates
[114] Department of Physics, New York University, New York NY; United States of America
[115] Ochanomizu University, Otsuka, Bunkyo-ku, Tokyo; Japan
[116] Ohio State University, Columbus OH; United States of America
[117] Homer L. Dodge Department of Physics and Astronomy, University of Oklahoma, Norman OK; United States of America
[118] Department of Physics, Oklahoma State University, Stillwater OK; United States of America
[119] Palacký University, Joint Laboratory of Optics, Olomouc; Czech Republic
[120] Institute for Fundamental Science, University of Oregon, Eugene, OR; United States of America
[121] Graduate School of Science, Osaka University, Osaka; Japan
[122] Department of Physics, University of Oslo, Oslo; Norway
[123] Department of Physics, Oxford University, Oxford; United Kingdom
[124] LPNHE, Sorbonne Université, Université Paris Cité, CNRS/IN2P3, Paris; France
[125] Department of Physics, University of Pennsylvania, Philadelphia PA; United States of America
[126] Department of Physics and Astronomy, University of Pittsburgh, Pittsburgh PA; United States of America
[127] [(a)] Laboratório de Instrumentação e Física Experimental de Partículas — LIP, Lisboa;[(b)] Departamento de Física, Faculdade de Ciências, Universidade de Lisboa, Lisboa;[(c)] Departamento de Física,

JHEP07(2023)125

Universidade de Coimbra, Coimbra;[(d)] *Centro de Física Nuclear da Universidade de Lisboa, Lisboa;*[(e)] *Departamento de Física, Universidade do Minho, Braga;*[(f)] *Departamento de Física Teórica y del Cosmos, Universidad de Granada, Granada (Spain);*[(g)] *Departamento de Física, Instituto Superior Técnico, Universidade de Lisboa, Lisboa; Portugal*

[128] *Institute of Physics of the Czech Academy of Sciences, Prague; Czech Republic*

[129] *Czech Technical University in Prague, Prague; Czech Republic*

[130] *Charles University, Faculty of Mathematics and Physics, Prague; Czech Republic*

[131] *Particle Physics Department, Rutherford Appleton Laboratory, Didcot; United Kingdom*

[132] *IRFU, CEA, Université Paris-Saclay, Gif-sur-Yvette; France*

[133] *Santa Cruz Institute for Particle Physics, University of California Santa Cruz, Santa Cruz CA; United States of America*

[134] [(a)] *Departamento de Física, Pontificia Universidad Católica de Chile, Santiago;*[(b)] *Millennium Institute for Subatomic physics at high energy frontier (SAPHIR), Santiago;*[(c)] *Instituto de Investigación Multidisciplinario en Ciencia y Tecnología, y Departamento de Física, Universidad de La Serena;*[(d)] *Universidad Andres Bello, Department of Physics, Santiago;*[(e)] *Instituto de Alta Investigación, Universidad de Tarapacá, Arica;*[(f)] *Departamento de Física, Universidad Técnica Federico Santa María, Valparaíso; Chile*

[135] *Department of Physics, University of Washington, Seattle WA; United States of America*

[136] *Department of Physics and Astronomy, University of Sheffield, Sheffield; United Kingdom*

[137] *Department of Physics, Shinshu University, Nagano; Japan*

[138] *Department Physik, Universität Siegen, Siegen; Germany*

[139] *Department of Physics, Simon Fraser University, Burnaby BC; Canada*

[140] *SLAC National Accelerator Laboratory, Stanford CA; United States of America*

[141] *Department of Physics, Royal Institute of Technology, Stockholm; Sweden*

[142] *Departments of Physics and Astronomy, Stony Brook University, Stony Brook NY; United States of America*

[143] *Department of Physics and Astronomy, University of Sussex, Brighton; United Kingdom*

[144] *School of Physics, University of Sydney, Sydney; Australia*

[145] *Institute of Physics, Academia Sinica, Taipei; Taiwan*

[146] [(a)] *E. Andronikashvili Institute of Physics, Iv. Javakhishvili Tbilisi State University, Tbilisi;*[(b)] *High Energy Physics Institute, Tbilisi State University, Tbilisi;*[(c)] *University of Georgia, Tbilisi; Georgia*

[147] *Department of Physics, Technion, Israel Institute of Technology, Haifa; Israel*

[148] *Raymond and Beverly Sackler School of Physics and Astronomy, Tel Aviv University, Tel Aviv; Israel*

[149] *Department of Physics, Aristotle University of Thessaloniki, Thessaloniki; Greece*

[150] *International Center for Elementary Particle Physics and Department of Physics, University of Tokyo, Tokyo; Japan*

[151] *Department of Physics, Tokyo Institute of Technology, Tokyo; Japan*

[152] *Department of Physics, University of Toronto, Toronto ON; Canada*

[153] [(a)] *TRIUMF, Vancouver BC;*[(b)] *Department of Physics and Astronomy, York University, Toronto ON; Canada*

[154] *Division of Physics and Tomonaga Center for the History of the Universe, Faculty of Pure and Applied Sciences, University of Tsukuba, Tsukuba; Japan*

[155] *Department of Physics and Astronomy, Tufts University, Medford MA; United States of America*

[156] *Department of Physics and Astronomy, University of California Irvine, Irvine CA; United States of America*

[157] *Department of Physics and Astronomy, University of Uppsala, Uppsala; Sweden*

[158] *Department of Physics, University of Illinois, Urbana IL; United States of America*

[159] *Instituto de Física Corpuscular (IFIC), Centro Mixto Universidad de Valencia — CSIC, Valencia; Spain*

[160] *Department of Physics, University of British Columbia, Vancouver BC; Canada*

[161] *Department of Physics and Astronomy, University of Victoria, Victoria BC; Canada*

[162] *Fakultät für Physik und Astronomie, Julius-Maximilians-Universität Würzburg, Würzburg; Germany*

JHEP07(2023)125

[163] Department of Physics, University of Warwick, Coventry; United Kingdom
[164] Waseda University, Tokyo; Japan
[165] Department of Particle Physics and Astrophysics, Weizmann Institute of Science, Rehovot; Israel
[166] Department of Physics, University of Wisconsin, Madison WI; United States of America
[167] Fakultät für Mathematik und Naturwissenschaften, Fachgruppe Physik, Bergische Universität Wuppertal, Wuppertal; Germany
[168] Department of Physics, Yale University, New Haven CT; United States of America

[a] Also Affiliated with an institute covered by a cooperation agreement with CERN
[b] Also at Borough of Manhattan Community College, City University of New York, New York NY; United States of America
[c] Also at Bruno Kessler Foundation, Trento; Italy
[d] Also at Center for High Energy Physics, Peking University; China
[e] Also at Centro Studi e Ricerche Enrico Fermi; Italy
[f] Also at CERN, Geneva; Switzerland
[g] Also at Département de Physique Nucléaire et Corpusculaire, Université de Genève, Genève; Switzerland
[h] Also at Departament de Fisica de la Universitat Autonoma de Barcelona, Barcelona; Spain
[i] Also at Department of Financial and Management Engineering, University of the Aegean, Chios; Greece
[j] Also at Department of Physics and Astronomy, Michigan State University, East Lansing MI; United States of America
[k] Also at Department of Physics and Astronomy, University of Louisville, Louisville, KY; United States of America
[l] Also at Department of Physics, Ben Gurion University of the Negev, Beer Sheva; Israel
[m] Also at Department of Physics, California State University, East Bay; United States of America
[n] Also at Department of Physics, California State University, Fresno; United States of America
[o] Also at Department of Physics, California State University, Sacramento; United States of America
[p] Also at Department of Physics, King's College London, London; United Kingdom
[q] Also at Department of Physics, Stanford University, Stanford CA; United States of America
[r] Also at Department of Physics, University of Fribourg, Fribourg; Switzerland
[s] Also at Faculty of Physics, Sofia University, 'St. Kliment Ohridski', Sofia; Bulgaria
[t] Also at Hellenic Open University, Patras; Greece
[u] Also at Institucio Catalana de Recerca i Estudis Avancats, ICREA, Barcelona; Spain
[v] Also at Institut für Experimentalphysik, Universität Hamburg, Hamburg; Germany
[w] Also at Institute for Particle and Nuclear Physics, Wigner Research Centre for Physics, Budapest; Hungary
[x] Also at Institute of Particle Physics (IPP); Canada
[y] Also at Institute of Physics, Azerbaijan Academy of Sciences, Baku; Azerbaijan
[z] Also at Institute of Theoretical Physics, Ilia State University, Tbilisi; Georgia
[aa] Also at Instituto de Fisica Teorica, IFT-UAM/CSIC, Madrid; Spain
[ab] Also at Istanbul University, Dept. of Physics, Istanbul; Türkiye
[ac] Also at L2IT, Université de Toulouse, CNRS/IN2P3, UPS, Toulouse; France
[ad] Also at National Institute of Physics, University of the Philippines Diliman (Philippines); Philippines
[ae] Also at Physics Department, An-Najah National University, Nablus; Palestine
[af] Also at Physikalisches Institut, Albert-Ludwigs-Universität Freiburg, Freiburg; Germany
[ag] Also at The City College of New York, New York NY; United States of America
[ah] Also at The Collaborative Innovation Center of Quantum Matter (CICQM), Beijing; China
[ai] Also at TRIUMF, Vancouver BC; Canada
[aj] Also at Università di Napoli Parthenope, Napoli; Italy
[ak] Also at University of Chinese Academy of Sciences (UCAS), Beijing; China
[al] Also at Yeditepe University, Physics Department, Istanbul; Türkiye

JHEP07(2023)125

[am] *Also at Institute for Nuclear Research and Nuclear Energy (INRNE) of the Bulgarian Academy of Sciences, Sofia; Bulgaria*
[*] *Deceased*

JHEP07(2023)125